

# Resilience of Spanish forests to recent droughts and climate change

Sacha Khoury  | David A. Coomes 

Forest Ecology and Conservation Group,  
Department of Plant Sciences, University of  
Cambridge Conservation Research Institute,  
Cambridge, UK

## Correspondence

David A. Coomes, Forest Ecology and  
Conservation Group, Department of  
Plant Sciences, University of Cambridge  
Conservation Research Institute, The David  
Attenborough Building, Cambridge CB2  
3QZ, UK.  
Email: dac18@cam.ac.uk

## Funding information

Cambridge Commonwealth, European &  
International Trust

## Abstract

A widespread increase in forest cover is underway in northern Mediterranean forests because of land abandonment and decreased wood demand, but the resilience of these successional forests to climate change remains unresolved. Here we use 18-year time series of canopy greenness derived from satellite imagery (NDVI) to evaluate the impacts of climate change on Spain's forests. Specifically, we analyzed how NDVI was influenced by the climatic water balance (i.e. Standardized Precipitation-Evapotranspiration Index, SPEI), using monthly time-series extracted from 3,100 pixels of forest, categorized into ten forest types. The forests increased in leaf area index by 0.01 per year on average (from 1.7 in 2000 to 1.9 in 2017) but there was enormous variation among years related to climatic water balance. Forest types varied in response to drought events: those dominated by drought-avoiding species showed strong covariance between greenness and SPEI, while those dominated by drought-tolerant species showed weak covariance. Native forests usually recovered more than 80% of greenness within the 18 months and the remainder within 5 years, but plantations of *Eucalyptus* were less resilient. Management to increase the resilience of forests—a key goal of forestry in the Mediterranean region—appears to have had a positive effect: canopy greenness within protected forests was more resilient to drought than within non-protected forests. In conclusion, many of Spain's successional forests have been resilient to drought over the past 18 years, from the perspective of space. Future studies will need to combine remote sensing with field-based analyses of physiological tolerances and mortality processes to understand how Mediterranean forests will respond to the rapid climate change predicted for this region in the coming decades.

## KEYWORDS

drought, greening, LAI, Mediterranean forest resilience, NDVI, protected areas, SPEI, time-series

## 1 | INTRODUCTION

An increase in the frequency, duration and/or severity of droughts associated with global warming is reshaping ecosystems in the Mediterranean (Fao & Plan Bleu, 2013). Forest die back has been

reported in some regions (Allen et al., 2010; Carnicer et al., 2011; Gómez-González, Ojeda, & Fernandes, 2018; Peñuelas et al., 2017). In other regions, however, studies have reported increases in forest biomass linked with land use changes and/or CO<sub>2</sub> fertilization. For instance, several remote sensing studies in Spain have

This is an open access article under the terms of the Creative Commons Attribution License, which permits use, distribution and reproduction in any medium, provided the original work is properly cited.

© 2020 The Authors. *Global Change Biology* published by John Wiley & Sons Ltd.

reported that forests are greening (Domingo, Javier, Paruelo Jose, & Miguel, 2008; Eastman et al., 2013; González-Alonso, Merino-De-Miguel, Roldán-Zamarrón, García-Gigorro, & Cuevas, 2006; Khorchani et al., 2018; Peñuelas, Filella, & Comas, 2002), despite warming (Gouveia, Bastos, Trigo, & Dacamara, 2012; Vicente-Serrano, Lopez-Moreno, et al., 2014), probably because successional processes following land abandonment are currently more influential than climate change in driving forest canopy dynamics (Carnicer et al., 2014; Martín-Alcón, Coll, & Salekin, 2015; Vayreda, Gracia, Martínez-Vilalta, & Retana, 2013). To our knowledge, nobody has yet attempted to disentangle the effects of forest succession and climate change on canopy greenness.

Quantifying, understanding and enhancing the resilience of forests to climate change are major areas of interest (Nimmo, Mac Nally, Cunningham, Haslem, & Bennett, 2015; Oliver et al., 2015), especially in the Mediterranean area which is undergoing a warming that exceeds the global trend at present and in most projections (Guiot & Cramer, 2016a). In Spain, enhancing forest resilience to drought has become a major goal of protected area management because the forests provide valuable ecosystem services including water regulation, timber and meat provision, regulation of climate and air quality, erosion control, as well as recreational and spiritual enjoyment (de la Guerra et al., 2017; Guiot & Cramer, 2016a; Scarascia-Mugnozza, Oswald, Piussi, & Radoglou, 2000; UNEP/MAP, 2016). Strategies for climate change adaptation used and proposed include favouring mixed species stands, reducing tree density, eliminating species with high water demands and introducing resilient species (de la Guerra et al., 2017). Given, however, how recent these management plans are, no studies have evaluated their effectiveness on a national scale, with the exception of Domingo et al. (2008), who compared greening trends inside and outside protected areas. Instead, researchers have focused on other ecosystem functions and services. A study evaluating multifunctionality in European protected areas found that in Spain those areas were associated with lower timber production and climate regulation functionality (van der Plas et al., 2018). Another study found that land use change in Europe's network of protected areas (i.e. Natura 2000), towards non-natural cover was greater than in non-protected areas, calling their effectiveness into question (Rodríguez-Rodríguez & Martínez-Vega, 2018). National-scale evaluation of the effectiveness of managing protected area for climate resilience was however absent and is therefore needed.

Understanding differences in the resilience of forest types is key to improving resilience to drought (Carnicer et al., 2011; Gavinet, Prévosto, & Fernandez, 2016; Machar et al., 2017; Martín-Alcón et al., 2015; Mochida, Saisho, & Hirayama, 2015; Ruiz-Benito, Lines, Gómez-Aparicio, Zavala, & Coomes, 2013; Yin & Bauerle, 2017). Multispectral imagery collected by earth observation satellites provide information on the greenness of pixels, which is linked to total canopy cover, leaf biomass and photosynthetic activity of the forest stand (Asrar, Myneni, & Kanemasu, 1989; Baret & Guyot, 1991; Carlson & Ripley, 1997; Cihlar, St.-Laurent, & Dyer, 1991; Tucker & Sellers, 1986; Zhang et al., 2003). Time-series of remote sensing data have been used to detect forest mortality (Coops, Johnson, Wulder, & White, 2006; Fraser & Latifovic, 2005; Garrity et al., 2013; Hart & Veblen,

2015; Ogaya, Barbeta, Başnou, & Peñuelas, 2015) and also canopy-level responses to drought event. For instance, Gazol et al. (2018) estimated the responses of 11 tree species to four drought events in Spain, in terms of satellite-derived canopy greenness (normalized difference vegetation index [NDVI]) and stem growth derived from dendrochronology. They recorded loss of greenness and growth during the drought events (i.e. sensitivity) and recovery following rain. The study found that recovery-to-sensitivity ratios varied greatly among the 11 species and along climate gradients: conifer-dominated woodlands in semi-arid regions were reported to be most sensitive to drought but recovered quickly while broadleaf-dominated woodlands in humid temperate regions were least sensitive to drought and recovered slowly. However, this study did not attempt to quantify long-term impacts, including the legacy of previous droughts (Anderegg et al., 2015; Gazol et al., 2018; Peltier, Fell, & Ogle, 2016).

Here, we evaluate one component of forest resilience to climate change—the ability of canopies to resist loss of leaves and/or recover leaves quickly—by looking at time-series of greenness alongside time-series of water availability. The analysis of remote sensing data over time is now possible over large scales thanks to advances in cloud computing technology and offers the opportunity to evaluate forest responses to drought in new detail. We analyse randomly sampled Spanish forest dominated by 10 species groups (i.e. forest types), inside and outside protected areas, to investigate canopy responses to the strong drought events and also the more subtle accumulation of drought stress through time. We address the following questions: (a) to what extent is the greening trend observed in Spanish forests being modulated by drought and climate change? (b) what environmental factors influence the response of canopy greenness to drought across Spain; (c) how does drought resilience vary among forest types and (d) do protected areas increase forests resilience to drought? Finally, we tested whether long-term trends in NDVI observed from space related to basal area trends measured in field inventories. A previous study from Spain found close agreement between ground- and remotely sensed estimates of NDVI when field estimates were made at the same spatial resolution as the remotely sensed pixel (Ogaya et al., 2015), and province-level averages of field and remotely sensed estimates of greenness were also in close agreement (González-Alonso et al., 2006). Here we extend this approach by comparing satellite imagery with field data collected by the Spanish National Forest Inventory.

Given the above-mentioned increases in aridity during the past decade and the evidence of forest die-back as well as greening in Spain, we expected to observe forest growth in some areas because of recent land abandonment and decline in areas that have recently become drier. In parallel, we expected that species-dominating areas that have always been dry, that is, south-east Spain, would be more resilient to drought than historically wetter areas. Concerning forest species' responses to drought, we envisaged that conifer canopies, specifically pines, would be less resilient to drought compared to broadleaf canopies because of reported succession advancement (Carnicer, Barbeta, Sperlich, Coll, & Peñuelas, 2013); and that non-native fast growing eucalypt would also be less resilient given their high water needs (Queirós et al., 2020). Finally, given that protected areas are supposed to be

managed for resilience, we expected them to respond differently to unprotected areas while recognizing that only 20%–50% are reported to have effective management (de la Guerra et al., 2017).

## 2 | METHODS

### 2.1 | Theory and definitions of resilience

Resilience to climate change has been defined in numerous ways and measured using many different approaches, making it hard to critically compare studies (e.g. Dakos, Carpenter, van Nes, & Scheffer, 2015; Hodgson, McDonald, & Hosken, 2015; Nimmo et al., 2015; Slette et al., 2019). Here we define resilience broadly as ‘the capacity of forest canopy to return to a state not qualitatively different from its pre-drought state by resisting and/or recovering’ (Folke et al., 2010; Hodgson et al., 2015). More specifically, we use the NDVI and leaf area index (LAI) as greenness and leaf area indices and the standardized precipitation evapotranspiration index (SPEI) as water availability indicator (Vicente-Serrano et al., 2017). The simplest resilience concept is illustrated in Figure 1e—here we see vegetation’s response to specific drought events—‘resistance’ is the capacity to withstand or tolerate drought, its opposite ‘sensitivity’ is computed here as the absolute loss in greenness during a drought event; ‘recovery’ and ‘adaptability’ are both computed here as the absolute gain in greenness following a drought event. We use a segmentation approach to detect these drought-related events (detailed in Section 2.6). We also develop an approach to quantify short-term and long-term resilience to drought (Camarero et al., 2018) based on measuring the correlation between greenness and water availability (Figure 1a–d; detailed in Section 2.5): here, short-term resilience is assessed by quantifying covariance (Figure 1c) and long-term resilience by comparing the observed greening trend with the potential greening trend (i.e. that predicted in the absence of climate change, Figure 1d). Remote sensing approaches are unable (currently) to measure the recruitment of new species and the loss of others, which may influence resilience via adaptation processes, these recruitment processes and shift in species distributions are therefore not addressed in this work (Folke et al., 2010).

### 2.2 | Site selection

Protected area maps were obtained from the Spanish Ministry of Agriculture, Food and Environment. We focussed on sampling locations categorized as Sites of Community Importance (known in Spain as Lugares de Importancia Comunitaria or LIC), and Special Conservation Zones (known in Spain as Zonas Especiales de Conservación or ZEC) within the Natura 2000 network, contrasting these sites with those without legal protection (Figure 2a). These sites include private and public lands that are meant to be managed in an ecologically and economically sustainable way, including agricultural activities, hunting and tourism (Martínez-Fernández, Ruiz-Benito, & Zavala, 2015). ZEC are supposed to be well-managed multifunctional

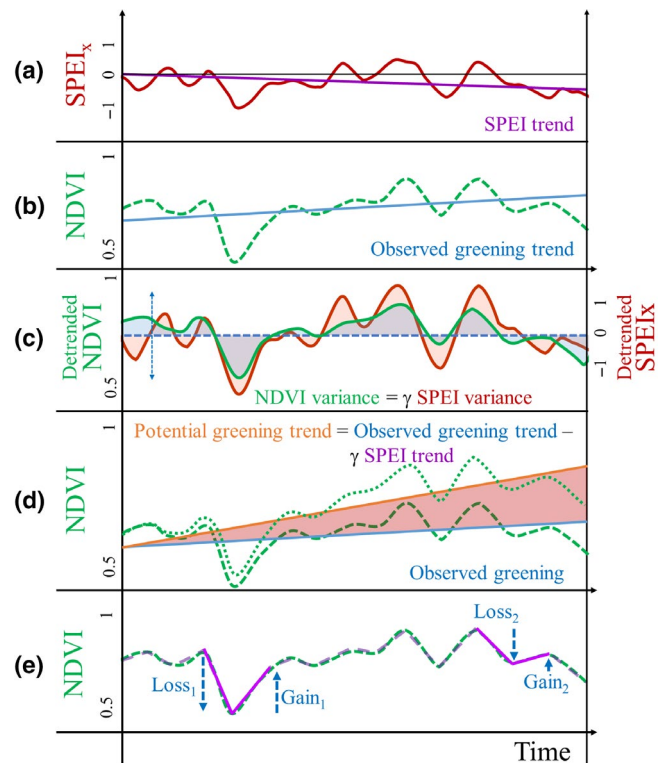


**FIGURE 1** Conceptual diagram explaining studied resilience measures: (a) A regression line (purple) is fitted to the standardized precipitation evapotranspiration index ( $SPEI_x$ ) time-series (dark-red) representing long-term climate changes; (b) a regression line (blue) is fitted to the deseasonalized time-series of normalized difference vegetation index (NDVI; dashed green) representing long-term change in greenness; (c) covariation is estimated between detrended NDVI (green) and detrended  $SPEI_x$  (red) from a linear model between the two; (d) deseasonalized time-series of potential greening (dotted green) and its corresponding trend (orange) are determined and the difference between potential and observed greening (shaded in red) corresponding to the long-term climate change influence on greenness; (e) to gain an alternative perspective, deseasonalized NDVI is segmented (dashed purple line) and two biggest negative changes representing forest canopy sensitivity (i.e. NDVI loss) are detected followed by the recovery measures (i.e. NDVI gain; solid purple segments)

woodlands that provide different ecosystem services, however as mentioned in the introduction, ecologically functional goals are not always achieved because of lack of proper management and funds. In 2017, 20%–50% of Natura 200 sites were LIC whose management plans were still under consideration for approval to become ZEC. Note that Nationally Designated Protected areas—which are concentrated in Catalonia and Andalusia—were omitted from the analyses because these are more strictly managed, usually prohibiting all human activity. It would be interesting to differentiate between Natura 2000 and Nationally Designated Protected areas in a future study.

Spain has the largest forest cover of any country in the Mediterranean with more than a quarter of its territory dedicated to nature conservation, and over 1,500 protected natural areas (FAO & Plan Bleu, 2013; de la Guerra et al., 2017). Stratified random

sampling was used to select 4,500 1-km<sup>2</sup> pixels representing 10 forest types and three protection statuses across Spain. In all, 10 dominant species groups (forest types) were considered for the analysis identified from European forest species distribution maps (Figure 2; Brus et al., 2012). We sampled 450 pixels randomly per forest type from areas that were over 60% forested selecting 10 of the most abundant species groups (Figure S2) as computed from species distribution maps by Brus et al. (2012). The dominant forest species dataset used includes broad taxonomic categories, some of which span several bio-climatic regions, such as oaks and maritime pines (Figure 2b).

Previous land cover could influence plant–water relations within sites because former farmland is likely to be on deeper soils, and that, in turn, could influence the resilience of forests. To test its influence, the land-cover type of each of our MODIS pixels was obtained by extracting data from the 1990 and 2000 CORINE Land Cover rasters (CLC2000\_CLC1990\_V2018\_20 and CLC2006\_CLC2000\_V2018\_20), and then downscaling from 100 to 500 m resolution using a nearest neighbourhood method (Figure S3: Corine 1990 and 2000 classifications for our pixels). Out of 4,500 pixels, 342 were classified as

agricultural, irrigated or non-vegetated lands in 1990 and 2000 years and were excluded because of inconsistencies with the map of Brus et al. (2012). Of the remainder, 304 (8.6%) were classified as ‘previously agricultural or irrigated land’ in 1990 and had transitioned to forest by 2000. We included previous land cover (i.e. agricultural vs forested in 1990) as a factor in our models.

## 2.3 | Time-series of greenness and drought severity

### 2.3.1 | Datasets

Monthly estimates of forest greenness in the form of NDVI (for the period February 2000–December 2017) were extracted from a NASA database (MODIS/006/MOD13Q1 & MODIS/006/MYD13Q1). NDVI was selected because it tracks seasonality more accurately than the Enhanced Vegetation Index and other indices (De Oliveira Silveira, De Carvalho, Acerbi, & De Mello, 2008; Evrendilek & Gulbeyaz, 2008; Verbesselt, Robinson, Stone, & Culvenor, 2009), but most importantly because NDVI resilience measures were shown to correlate

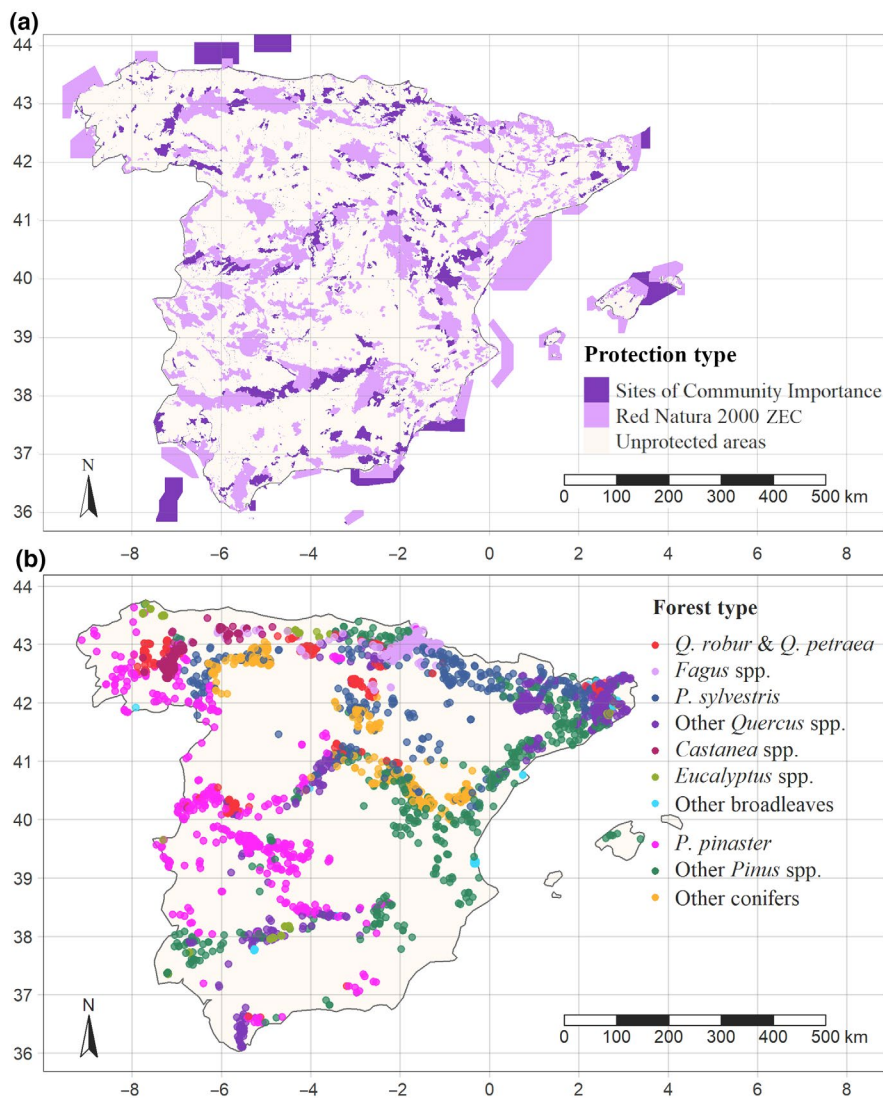


**FIGURE 2** Study site selection. (a) Protected areas considered in this study; (b) dominant species of pixels extracted taken from Brus et al. (2012). Note that the ‘other broadleaves’ category represents planted woodlands dominated by species such as almond, carob, elm, lemon, poplar, whereas ‘other conifers’ represent species such as cedars and junipers

with tree-ring derived resilience measures (Gazol et al., 2018). The dataset comprises multispectral reflectance measurements recorded by MODIS Aqua and Terra satellites at a spatial resolution of 250 m (Didan, 2015a, 2015b), from which 16-day composites were constructed. These data have been corrected for atmospheric and bi-directional surface reflectance effects, and water, clouds, heavy aerosols and cloud shadows have been masked out by Nasa. We further masked time-series of NDVI following quality assurance information and aggregated to monthly values at the resolution of 500 m. LAI was also obtained from MODIS product MODIS/006/MCD15A3H for the year 2013 at 500 m resolution (Myneni, Knyazikhin, & Park, 2015) to relate losses and gains in greenness to biomass on the ground. Summary data were exported for analysis in R. It is known that NDVI and LAI are nonlinearly related, with NDVI saturating at high LAI (Figure S4), and this nonlinearity is considered when interpreting results (Le Maire et al., 2006; Turner, Cohen, Kennedy, Fassnacht, & Briggs, 1999). A nonlinear model was fitted to average NDVI for the year 2013 with average LAI, and the model was used to convert NDVI time-series into LAI time-series and interpret all results obtain from NDVI analysis in LAI terms as well (Table S1, M5; Figure S4).

An absolute measure of yearly climatic water balance was computed for each site to evaluate the effect of the latitudinal climatic gradient on forest response to drought. It corresponds to monthly precipitation minus potential evapotranspiration averaged across the 18 years. Potential evapotranspiration was calculated using the 'Penman' function in the SPEI package (Beguería & Vicente-Serrano, 2017), by inputting minimum and maximum temperature, mean daily external radiation, wind speed and pixel latitude. All climatic variables were extracted from Global Land Data Assimilation System 2.1 products (Rodell et al., 2004). In addition, time-series of monthly absolute water balance were also used to be compared with the relative water balance index, SPEI (used in this paper to evaluate the intensity of drought).

Elevation data were obtained from the Shuttle Radar Topography Mission digital elevation dataset, version 4 (Jarvis, Reuter, Nelson, & Guevara, 2008).

Time-series of SPEI, representing relative water availability, were extracted from a database available at 1.1 km resolution for the entirety of Spain from 1961 to 2017, and used as a climate change index (Vicente-Serrano et al., 2017). It is important to note that SPEI provides an index of temporal change in water availability within a site. It should not be used to make direct comparisons of absolute water availability among sites but can be used to compare the relative intensity of a dry or wet period. For example, in this paper, we are mostly interested in the severity of drought events relative to the severity of drought events experienced over time in a site and use this relative severity (i.e. SPEI) when comparing forest responses. SPEI is widely used as an alternative to SPI, which is based solely on precipitation (Azorin-Molina et al., 2014; Bottero et al., 2017; Gazol et al., 2018; Tejedor, de Luis, Cuadrat, Esper, & Saz, 2016; Vicente-Serrano, Beguería, & López-Moreno, 2010). SPEI is computed as follows: first, a monthly water balance is calculated for every month from 1961 to 2017, by subtracting weekly potential evapotranspiration from weekly precipitation. Second, because the impacts of drought can be cumulative, a

sequence of alternative SPEI time-series is created from SPEI values averaged over a different number ( $X$ ) of months. In this study, SPEI is calculated for  $X$  ranging from 1 to 48 months. The cumulative water balance is calculated from the weighted average of a particular month and the  $X - 1$  previous months using a rectangular weighing function. The  $SPEI_X$  is then obtained from normalizing water balance series into a three-parameter log-logistic distribution using non-biased probabilistic weighted moments to calculate the parameters. The parameter estimation of the log-logistic probability distribution and detailed calculation procedure for SPEI index can be found in Vicente-Serrano et al. (2010). The result is a non-seasonal time-series of  $SPEI_X$  values that represent the probability of a given month being relatively dry or wet compared to the reference period 1961–2014 (Beguería, Vicente-Serrano, Reig, & Latorre, 2014; Mckee, Doesken, & Kleist, 1993; Vicente-Serrano et al., 2010). Given that the Spanish drought dataset consisted of four SPEI time steps per month (Vicente-Serrano et al., 2017), we averaged those four values to get time-series of monthly SPEI.

Datasets mentioned in this section, with the exception of SPEI, were all available through Google Earth Engine.

### 2.3.2 | Greening and climate change trends

A particularly effective method of monitoring vegetation from space is detecting and understanding changes in time-series of greenness (Jamali, Jönsson, Eklundh, Ardö, & Seaquist, 2015). These changes tend to fall under three categories: seasonal changes, gradual changes and abrupt changes (Verbesselt, Hyndman, Newnham, & Culvenor, 2010). Recent methods of analysing these changes consist of decomposing the time-series into 'trend' which captures the gradual changes caused by interannual climate and land use variations as well as the abrupt changes cause by disturbances, 'seasonality' which follows annual temperature and rainfall, and 'remainder' variations unexplained by the former factors (Jamali et al., 2015; Verbesselt et al., 2010). In this work, we focus only on gradual changes in NDVI and LAI trend, which are the type of change that drought usually causes. In this first part we deseasonalized the NDVI time-series to relate it to non-seasonal climate change index SPEI using the DBEST package in R (Jamali et al., 2015; Jamali & Tomov, 2017). The DBEST function detected abrupt changes in 20 of the 4,158 pixels, which were excluded from subsequent analyses as they represent extreme events such as fire, clear-felling and sensor-related artefacts which are beyond the scope of our study. A further 952 plots were eliminated because of missing NDVI or SPEI data-points leaving 3,528 plots for further analysis. We used two linear models (Table S1, M1 and M2) to determine trends in SPEI and greenness over the past 18 years:

$$SPEI_X(t) = \beta_C + \alpha_C \cdot t + \varepsilon_C(t), \quad (1)$$

$$NDVI(t) = \beta_G + \alpha_G \cdot t + \varepsilon_G(t), \quad (2)$$

where  $t$  is time (1 to 215 months) within the 18-year time-series,  $\alpha$  and  $\beta$  are coefficients estimated by least-squares regression and  $\varepsilon$

are normally distributed residuals. Subscripts in these models indicate C for climate and G for observed greenness.  $\beta$  is the predicted initial SPEI<sub>X</sub> or NDVI of a plot (i.e. on February 2000), and  $\alpha$  represents the long-term linear trend in climate (i.e. SPEI) or greenness of a plot, respectively.

Further linear models were used to evaluate how greening trends vary across Spain, testing whether they vary with elevation, average water balance, average greenness, forest type and protection status (Table S1, model M10–M11). Models were conducted using spatial simultaneous autoregressive error estimation (SSAEM), which account for the residual spatial structure within the neighbourhood of pixels (*spatialreg* package in R; Bivand & Piras, 2019). AIC and correlograms at varying neighbourhood distances were used to determine the best-supported model to account for spatial autocorrelation.

## 2.4 | Determining the drought accumulation period across Spanish forests

To determine the drought accumulation period over which drought affects forest greenness, we recorded which SPEI<sub>X</sub> time-series correlated most closely with the forest greenness time-series at a site. We used a cross-correlation function with zero time lag (as the X scales of SPEI are already computed to account for time lags) correlating detrended SPEI<sub>X</sub> against detrended, deseasonalized NDVI for drought accumulation periods ranging from X = 1 to 48 months, and the value of X that gave rise to the highest correlation was noted: we refer to this as the drought accumulation period, and this period was used in all subsequent analyses. This allowed us to account for lags in forest response to drought and delayed mortality to which some species are susceptible, and for different water reservoirs that cause a delay in water deficit and surplus effects (Vicente-Serrano et al., 2013).

## 2.5 | Time-series analysis of forest response to drought

SPEI<sub>X</sub> and NDVI time-series were used to quantify two metrics for each pixel: short-term covariance and long-term climate change influence (CCI; see Figure 1). A linear model (Table S1, M4) was fitted to the deseasonalized NDVI time-series using smoothed SPEI<sub>X</sub> time-series, where deseasonalization was achieved using the DBEST package, and smoothing using locally weighted smoothing ( $\theta = 0.1$ ) in R, to eliminate noise and make SPEI<sub>X</sub> comparable to the NDVI trend:

$$\text{NDVI}(t) = \alpha_G \cdot t + \gamma_G \text{SPEI}_X(t) + \beta_G + \varepsilon_G(t), \quad (3)$$

where  $t$  is time (1–215 months) within the 18-year time-series,  $\alpha_G$ ,  $\beta_G$  and  $\gamma_G$  are coefficients estimated by least squares regression and  $\varepsilon_G$  is the residual. Subscripts in these models indicate P for potential greenness and G for observed greenness.

Substituting Equation (1) into Equation (3) we get:

$$= \alpha_G \cdot t + \gamma_G (\alpha_C \cdot t + \beta_C + \varepsilon_C(t)) + \beta_G + \varepsilon_G(t).$$

This is reorganized to give:

$$= \alpha_P \cdot t + \beta_P + \varepsilon_P(t), \quad (4)$$

where  $\alpha_P = \alpha_G - \gamma_G \cdot \alpha_C$ ,  $\beta_P = \beta_G - \gamma_G \cdot \beta_C$ , and  $\varepsilon_P = \varepsilon_G - \gamma_G \cdot \varepsilon_C$ . Here  $\alpha_P$  is the potential greening trend; it is comprised of the observed greening trend  $\alpha_P$  and the influences of long-term changes in climate ( $\gamma_G \cdot \alpha_C$ ) on greenness.  $\gamma_G$  provides an estimate of how strong the covariance between greenness and changes in water availability (CGW) is  $\alpha_G - \alpha_P = \gamma_G \cdot \alpha_C$  corresponds to estimated long-term CCI on greenness.  $\varepsilon_G$  is the residual which contains the nonlinear trend, the seasonality and the noise (also normally distributed).

Regression modelling produces two new summary variables for each pixel: short-term CGW and long-term CCI. It is key to understand that CGW, represented by the coefficient ' $\gamma$ ' in Figure 1c which quantifies how greenness varies with drought index on a monthly basis, relates to both losses and gains and is not an indication of resilience alone. Large CGW values correspond with big losses and/or big gains. Strong and weak covariance could indicate different mechanisms to overcome droughts better known as drought avoidance and drought tolerance mechanisms, respectively, which relate to anisohydric and isohydric behaviours (Hwang et al., 2017; Roman et al., 2015; Sade, Gebremedhin, & Moshelion, 2012). CCI, on the other hand, represents the long-term CCI on greenness; it can be represented as the difference between the actual greenness and the potential greenness as demonstrated in Figure 1d if greenness in the long term is affected to similar degree to the short term by the coefficient ' $\gamma$ '.

Statistical modelling was used to evaluate how short-term covariance and long-term CCI varied across Spain, in relation to elevation, average water balance and average greenness (Table S1, M14–M21). Additional models included forest type and protection status as explanatory variables.

We evaluated whether field data confirmed remote sensing analyses at the national scale using the Spanish National Forest Inventory, albeit with plots that differed in resolution from the satellite data. The Spanish Forest Inventory is a systematic network of plots each km<sup>2</sup> of forested areas in Spain (Villaescusa & Díaz, 1998; Villanueva, 2004). For basal area calculations, we used the permanent plots between the third (1997–2007) and fourth (1998–2008) survey but excluded plots measured before 2000. Each plot has a variable radius design, comprised of four concentric circular subplots of 5, 10, 15 and 25 m where adult trees of <12.5, <22.5, <42.5 and ≥42.5 were measured, respectively. For each sampled tree, it was recorded status (alive, death), height, d.b.h., and species identity. Basal area change was computed as the difference in stand basal area in m<sup>2</sup>/ha between the two surveys (Ruiz-Benito et al., 2013). Given the very different spatial resolution of the MODIS data (500 m) and the field plots (25 m), we

restricted our analyses to pixels in which forest was relatively homogeneous. To do this, a cloud-free image of Spain was obtained (by mosaicking Sentinel-2 level 1C images from May to August 2016) and NDVI computed for pixels of 25 and 500 m resolution centred on the plot locations. Sites which had a difference in NDVI over 0.01 between the two resolutions were excluded from further analyses leaving 2,150 out of 4,649 pixels/plots to analyse. Modis NDVI data were extracted using the approach described in Section 2.3.1 and the absolute NDVI trend (determined from the DBEST package) was computed between the dates of the third and fourth national forest inventory. Spatial autoregressive modelling was used to determine the relationship between the greenness and basal area change.

## 2.6 | Breakpoint analysis approach to resilience estimation

Breakpoint analyses were conducted to detect the greatest changes in NDVI and LAI within each time-series, from which loss and gain indices were estimated. The time-series NDVI and LAI were decomposed

into trend, seasonality and remainder (see Section 2.3.2), and the trend segmented using the DBEST package in R (Jamali & Tomov, 2017). As illustrated in Figure 1e, loss and gain were estimated from the two most negative segments followed by a positive segment, respectively. Loss was estimated as the mean of the absolute negative changes in NDVI (i.e.  $NDVI_{peak} - NDVI_{pre-event}$ ) and gain as the mean increase in NDVI following these negative changes (i.e.  $NDVI_{post-event} - NDVI_{peak}$ ). Minimum water availability (minimum SPEI) as well as maximum water availability (maximum SPEI) were extracted over those two detected loss and gain periods, respectively, and their mean computed for each series, representing water deficit and water surplus events, respectively. Spain experienced major droughts in 2005, 2012 and 2017 (Figure 4a), we selected only the two biggest declining segments before March 2014—allowing time for recovery—to estimate forest resilience components. We did not examine specific years or months because drought intensity varies over space and time. Instead, we determined the water availability at times when major losses and gains in NDVI or LAI were detected in the time-series, therefore allowing droughts starting dates to vary. Nevertheless, drops in NDVI and LAI were mostly associated with the two drought years of 2005 and 2012 (Figure S5).

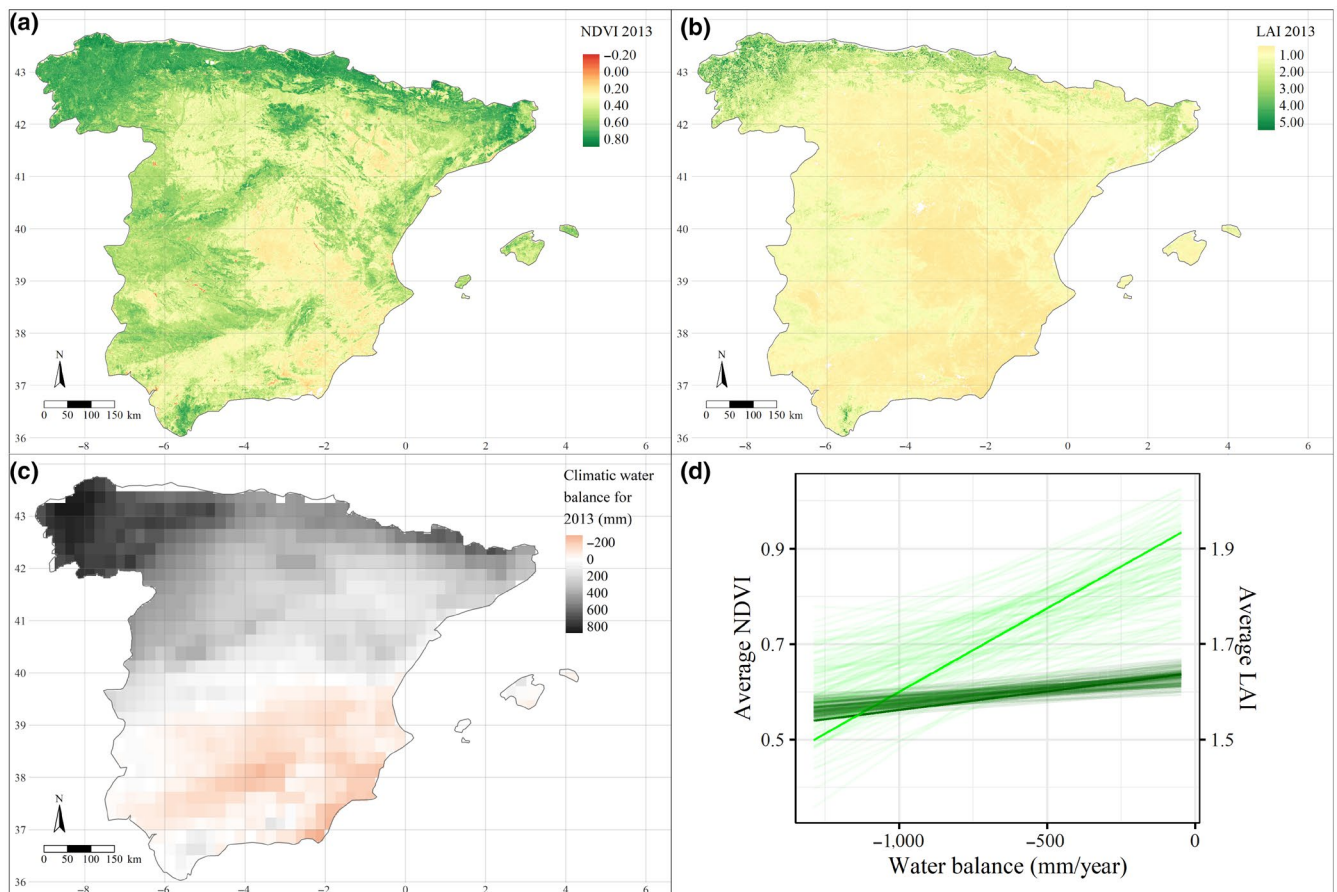


**FIGURE 3** Greenness and water availability landscape in Spain. (a) Average normalized difference vegetation index (NDVI) over Spain for the wet year of 2013; (b) average leaf area index (LAI) over Spain for 2013; (c) average climatic water balance as computed from difference between monthly precipitation and Thornthwaite potential evapotranspiration for 2013; (d) variation in average greenness and canopy cover with average yearly water balance (mm/year). NDVI regression line in dark green and LAI regression line in bright green with uncertainty around these lines shaded in green

To determine the relationships between loss and gain, and to test whether it varied systematically among forest types and protection statuses, we used ordinary least-square regression. Loss and gain were log-transformed to improve residual normality (Table S1, model M5; Figure 10a; Figure S6). Predictions were then back-transformed to arithmetic scale with a correction factor (Figure 10a; Figure S6; Baskerville, 1972).

To help elucidate the drivers of resilience, losses and gains in greenness and leaf area, and their ratio estimate, were modelled as a function of elevation, average water balance, average greenness, relative water deficit (-minimum SPEI), water surplus (maximum SPEI), forest type and protection status again using SSAEM (Table S1, M22–M39).

## 3 | RESULTS

### 3.1 | Water balance is the biggest determinant of forest greenness and leaf area

As expected, forests were greenest in the wetter regions of Spain (Figure 3d), with greenness (i.e. average NDVI) and canopy cover (average LAI) varying with environment as follows (coefficients in bold are significant at  $p < .01$ ):

$$\text{Mean NDVI} = \mathbf{0.64} + \mathbf{0.000054} [\text{water balance}] ;$$

standard error ( $SE$ ) = 0.014 and 0.000014, respectively.

$$\text{Mean LAI} = \mathbf{1.88} + \mathbf{0.00022} [\text{water balance}] ;$$

$SE = 0.090$  and  $0.00008$ , respectively.

### 3.2 | Long-term trends in water availability and greenness

Over the past 18 years, 73% of Spanish land has become drier, with an average change in  $\text{SPEI}_1$  of  $-0.24$ , indicating the mean, which is almost a quarter of a standard deviation drier than the average for 1961 to 2014 (Figure 4). This corresponds to an increase in water deficit of about 2 mm/year as calculated from the linear relationship between  $\text{SPEI}_1$  and water balance (Figure 4c). Of the forest pixels that we randomly sampled over Spain (Figure 2b), 35% showed a significant drying trend (linear modelling,  $p < .05$ ), 37% did not change significantly and 27% got wetter (Figure 5a). The climate of the wetter regions changed least while the drier regions became increasingly arid (i.e. Figure 4b,c).

Despite these strengthening water deficits, 75% of Spanish forest pixels became greener over time and only 12% became less green (Figure 5b). On average there was a 11% increase in LAI (from 1.7 to 1.9  $\text{m}^2/\text{m}^2$ ), and some variation with canopy density (i.e. average LAI): less green sites (lower quartile LAI = 1.36) accumulated 0.1  $\text{m}^2/\text{m}^2$  of leaf area while the more green sites (upper quartile LAI = 2.26) accumulated 0.3  $\text{m}^2/\text{m}^2$  over 18 years (Figure 6).

Correlation of remote- and plot-based observations of forest change (see Section 2.5 for details) showed a significant positive logarithmic relationship between basal area and average deseasonalized

NDVI at the time of the third inventory, with a Nagelkerke  $R^2$  of .22 (Figure 3a). A significant positive linear relationship was found between basal area change and NDVI trend change between the two inventories (Figure 3b) with a Nagelkerke  $R^2$  of .12. These analyses build confidence that our remote sensing analyses of resilience correspond with changes observed on the ground.

Examining individual time-series, we found a close covariance of greenness with climatic conditions:  $\text{SPEI}_x$  explained 49% of the variation in canopy greenness (average  $R^2$  of 3,182 linear models fitted to paired  $\text{SPEI}$ -NDVI time-series). Only 19% of the pixels responded immediately to water deficit (i.e. correlated best with a drought accumulation period  $X$  of only 1 month).

In the long term, CCI on greenness was significant in 58% of the plots (with 56% negative effects and 2% positive effects,  $p < .05$ ) but changes were small in magnitude (Figure 7). The CCI on NDVI varied across Spain as follows (Figure 7a) (coefficients in bold are significant at  $p < .01$ ):

$$\text{CCI}_{[\text{NDVI}]} = \mathbf{-0.0016} + \mathbf{0.0023} [\text{water balance}] + \mathbf{0.0010} [\text{elevation}] ,$$

$SE = 0.0005, 0.0004$  and  $0.0003$ , respectively.

To put this model in context, on average canopy greenness was observed to increase by 0.0274 over 18 years, assuming a linear relationship between NDVI and  $\text{SPEI}$  trends, our model predicts increase of 0.0284 if climate change had not occurred. The equation shows that climate change did have a stronger impact at dry sites and at low elevation (Figure 7a). Similarly, the CCI on LAI (Figure 7b) is given by (coefficients in bold are significant at  $p < .01$ ):

$$\text{CCI}_{[\text{LAI}]} = \mathbf{-0.0015} + \mathbf{0.0121} [\text{water balance}] + \mathbf{0.0075} [\text{mean LAI}] ,$$

$SE = 0.0038, 0.0031$  and  $0.0019$ , respectively.

$\text{CCI}_{[\text{LAI}]}$  increased from  $-0.020$  at the driest sites to 0.017 at the wettest sites (i.e. from  $-1,181.5$  to  $-301.5$  mm, these representing the 5th and 95th percentiles of observed distribution in annual water balance). It also increased with LAI from  $-0.013$  at 0.88 to 0.011 at 2.93 (again the 5th and 95th percentiles of LAI). Again, this means that the CCI on greenness caused the LAI trend to be significantly smaller in drier or more dense sites (Figure 7b).

### 3.3 | Water availability is the main driver of short-term changes in forest greenness

The short-term effect of climatic variation on canopy greenness (CGW, see Section 2.5) varied across Spain as follows (Figure 8) (coefficients in bold are significant at  $p < .01$ ):

$$\text{CGW}_{[\text{NDVI}]} = \mathbf{0.0148} - \mathbf{0.0041} [\text{mean NDVI}] - \mathbf{0.0034} [\text{elevation}] ,$$

$SE = 0.0008, 0.0003$  and  $0.0004$ , respectively.

The terms in square brackets are scaled environmental variables. The model demonstrates that the covariance was weaker in elevated areas. The covariance was also weaker in forest with high NDVI but

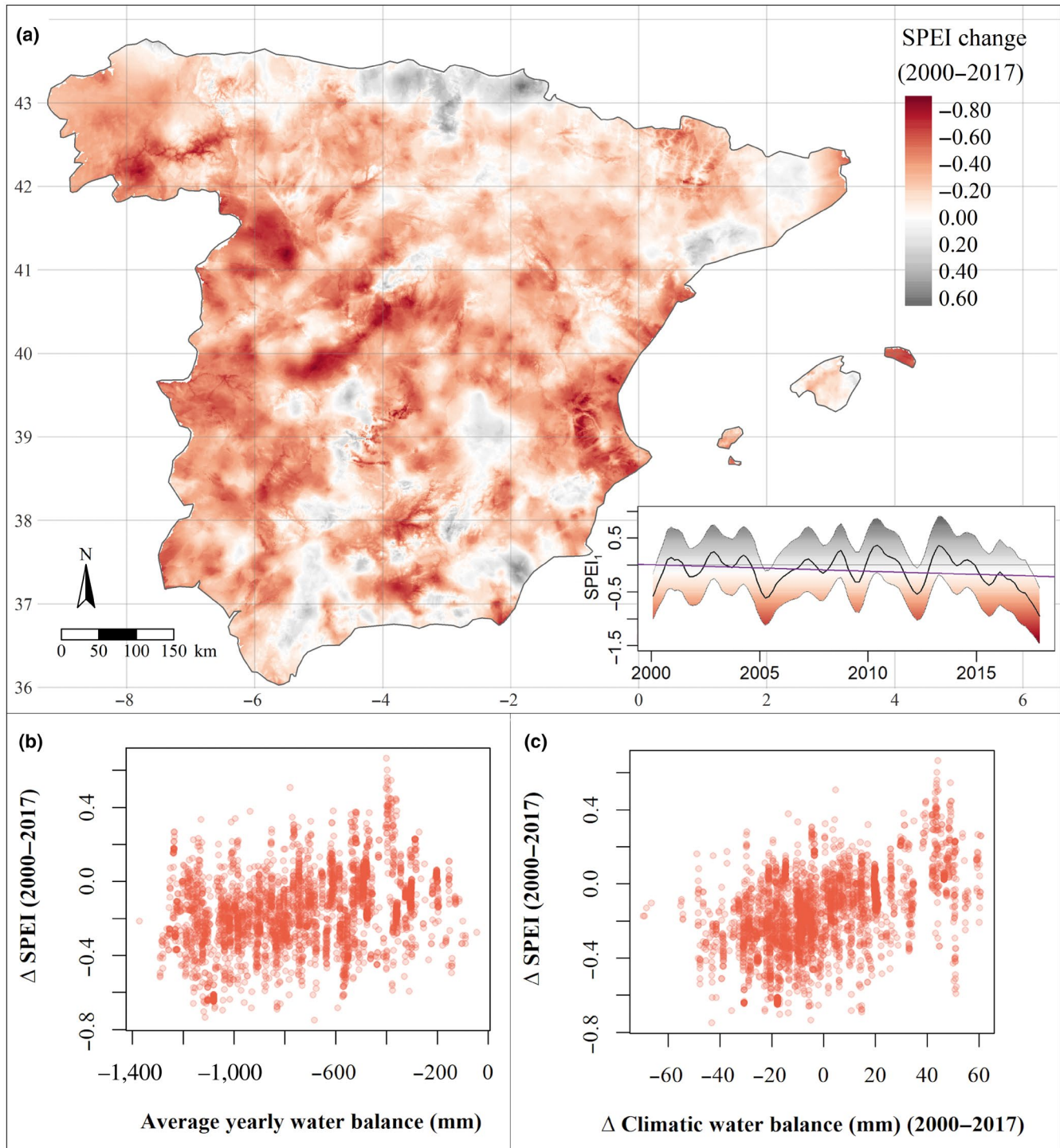


**FIGURE 4** Standard Precipitation-Evapotranspiration Index (SPEI) over Spain. (a)  $SPEI_1$  change over Spain for the period 2000–2017; with the inset showing the average  $SPEI_1$  over Spain  $\pm$  standard deviation and linear trend in purple; (b) relationship between SPEI change and average water balance, computed from the Penman–Monteith equation (see S2:M6); (c) relationship between SPEI change and yearly water balance change over the past 18 years (see S2:M7)

once the result was converted to LAI, it translated into a stronger covariance for forest with denser canopies (i.e. large LAI) (coefficients in bold are significant at  $p < .01$ ):

$$CGW_{[LAI]} = \mathbf{0.0918} + \mathbf{0.0262} [\text{mean LAI}] - \mathbf{0.0222} [\text{elevation}],$$

with  $SE = 0.0052, 0.0018$  and  $0.0023$ , respectively.

Breakpoint analysis demonstrated that in aftermath of a strong drought event, forests regained, on average, only 80% of their lost greenness during droughts. Given that forests accumulated leaf area over the 18-year study, they must have regained the remaining 20% of their leaves (and more) in subsequent years not captured by the analyses' characterization of losses and gains. Losses

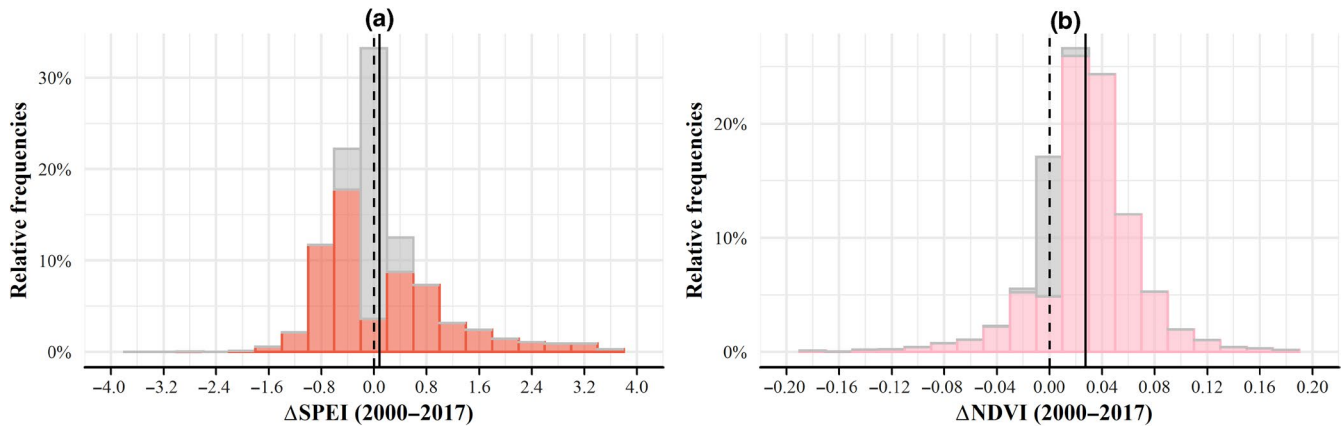


**FIGURE 5** Changes in Standard Precipitation-Evapotranspiration Index (SPEI) and greenness over the past 18 years in studied Spanish forests: (a) Relative frequency histogram of  $\Delta\text{SPEI}_x$  change over forest plots with significant changes in red and non-significant changes in grey (linear modelling,  $p < .05$ ); (b) relative frequency histogram of changes in greenness over forest plots with significant changes in pink and non-significant changes in grey (linear modelling,  $p < .05$ ). Black lines indicate average of change in SPEI and normalized difference vegetation index

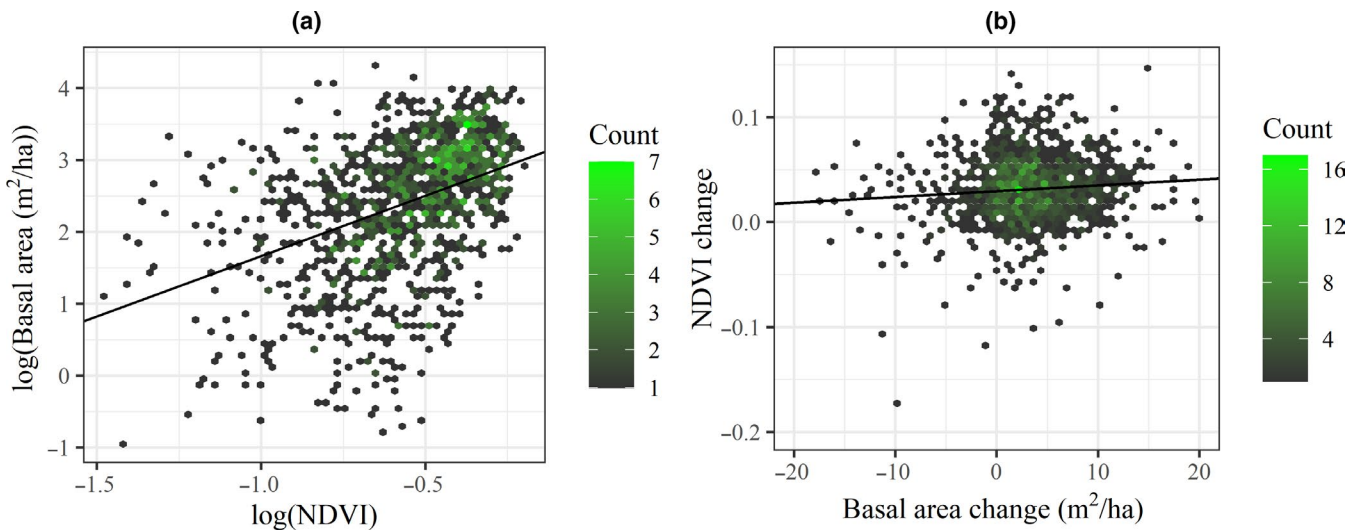


**FIGURE 6** Relationship between plot-based measurements of basal area and remotely sensed measurements of greenness. (a) Basal area measured during the third Spanish national forest inventory as a function of average deseasonalized normalized difference vegetation index (as extracted from DBEST) for the same date; (b) greenness change as a function of basal area change between the third and fourth Spanish national forest inventory

and gains in LAI were greatest in dry regions (Figure 9(1)). The relative water deficit during a drought event (-minimum SPEI) and relative water surplus post drought (maximum SPEI) both had a significant effect on all resilience components. The canopy greenness losses and gains were greater with an increase in water deficit (Figure 9a,b(2)). Furthermore, pixels hit by stronger drought were more resilient as deduced from the water deficit negative relationship to the gain-to-loss ratio (Figure 9c(2)). The NDVI gain, as well as gain-to-loss ratio, were equally affected by how wet the period that followed the drought was (Figure 9b,c(3)). Denser forests (i.e. forest with higher LAI) lost and gained more due to droughts (Figure 9(5)). Forests at higher elevation were more resistant to drought events (Figure 9a(5)).

### 3.4 | Influences of forest type on drought response

Forests exhibited a spectrum of responses to drought, with breakpoint analysis indicating that some forest types lost and re-gained little NDVI or LAI while others fluctuated greatly (Figure 10a). Gains and losses were correlated across forest types ( $r = 0.66$  for NDVI and  $r = 0.48$  for LAI; Figure 10a). Specifically, *Castanea*-dominated forests had below-average losses and gains indicative of drought tolerance while maritime pines had above-average losses and gains indicative of drought avoidance (Figure 10a). This range of responses was confirmed by the analyses of the entire time-series; there was a close correlation between the short-term covariance of

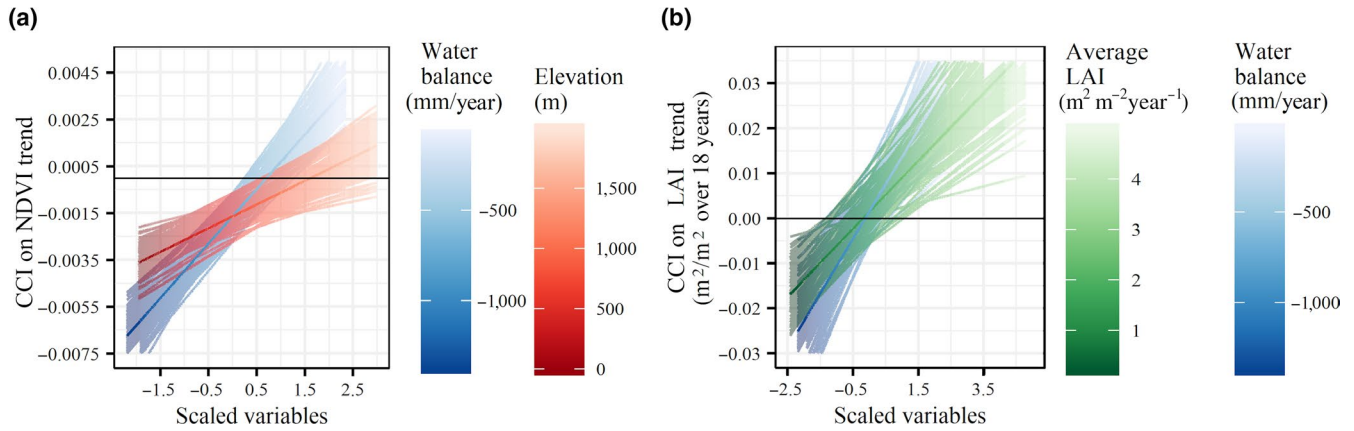


**FIGURE 7** Climate change influence (CCI) on greenness (i.e. difference in greenness trend cause by long-term trends in climate), as a function of elevation (m), water balance (mm/year) and average LAI ( $m^2 m^{-2} year^{-1}$ ). (a) CCI as computed from modelling normalized difference vegetation index with Standard Precipitation-Evapotranspiration Index (SPEI) as function of environmental variables; (b) CCI as computed from modelling LAI with SPEI as function of environmental variables. Uncertainty around regression lines is shaded in the environmental variable respective colour

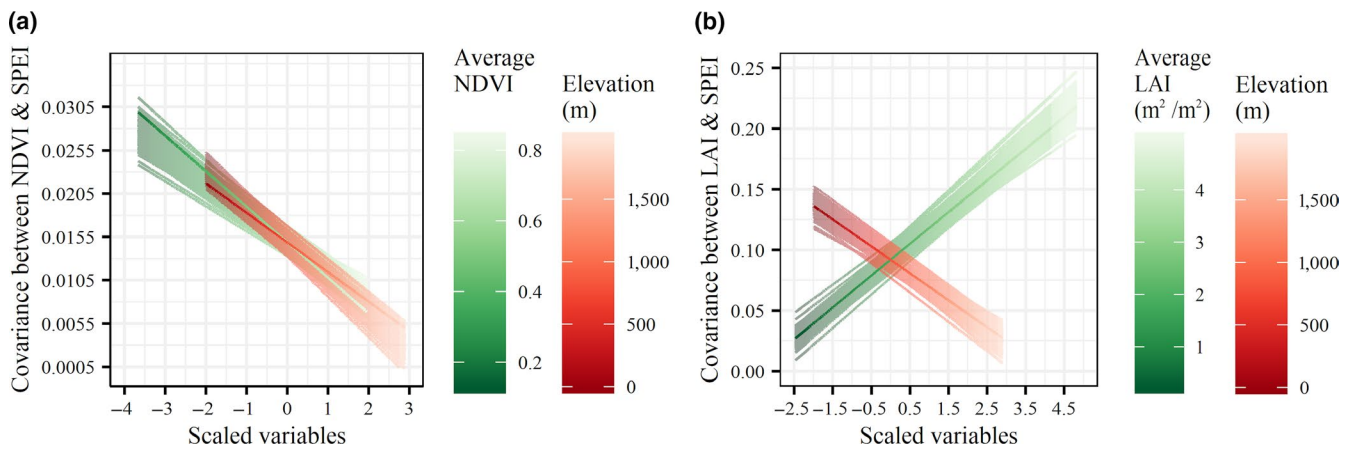


**FIGURE 8** Variation of short-term covariance between greenness and Standard Precipitation-Evapotranspiration Index (SPEI) along forest density and elevation gradients. (a) Covariance between normalized difference vegetation index and SPEI; (b) covariance between LAI and SPEI. Uncertainty around regression lines is shaded in the environmental variable respective colour

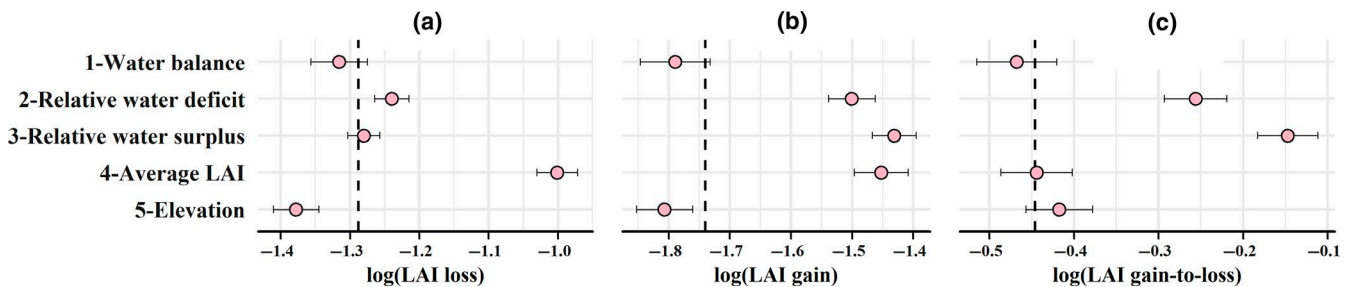


**FIGURE 9** Effects of environmental conditions on (a) loss during drought; (b) gain after drought and (c) gain-to-loss ratio of LAI. The effect sizes shown are coefficients (mean  $\pm$  99% confidence intervals) estimated by spatial autoregressive modelling. Explanatory variables are scaled, so coefficients indicate the effect on these components of shifting to an environment that is +1 SD from the mean environment. The dashed lines indicate the average loss, gain and gain/loss ratio for the mean environment

greenness and SPEI, and the greenness gains and losses determined by breakpoint analysis within the different forest types (Figures S13 and S14). Species groups that lost and gained

little after drought had a lower short-term CGW while species groups that lost and gain a lot had higher short-term CGW (indicated by circle sizes in Figure 10a); short-term covariance

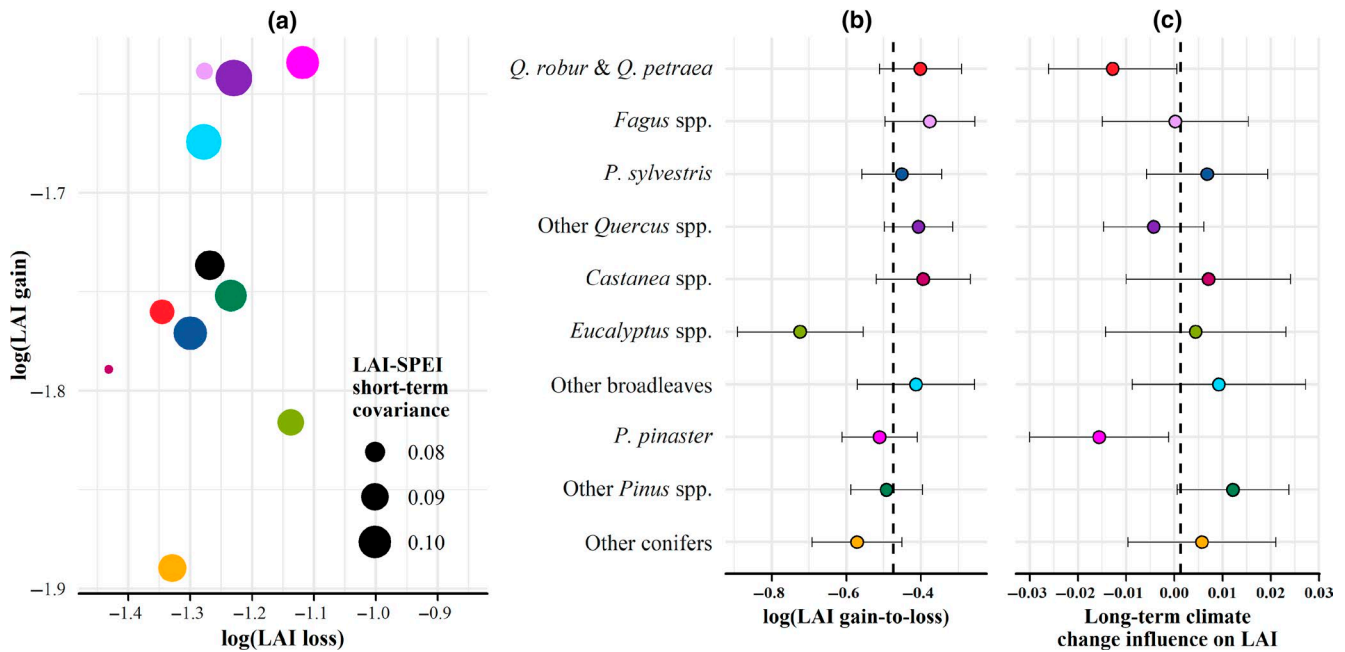


**FIGURE 10** Summary coefficients for the forest types of the spatial autoregressive model performed to evaluate resilience components. (a) Relationship between the loss, gain and the short-term response to drought of forest types; (b) gain-to-loss ratio (log scale) and (c) long-term climate change influence on greenness. Value for forest type indicates mean response for forests outside of protected areas. Overall mean for forest outside protected areas indicated by the black dot in (a) and the dashed lines in (b) and (c), and the error bars represent 99% confidence intervals. Note losses and gains were log transformed to improve normality of residuals, since both measurements are right skewed, and because gains tend to be smaller when losses are large

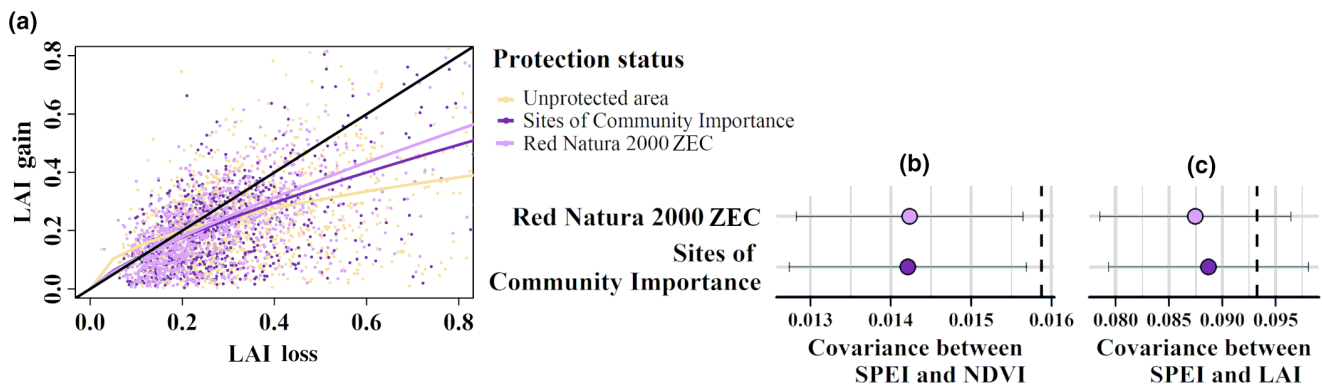


**FIGURE 11** Leaf area losses and gain in the short term across different protection statuses. (a) LAI losses and gains to severe droughts with fitted line back transformed from the log-log relationship between the two; (b) summary coefficients for the protected areas of the spatial autoregressive model performed to evaluate short-term covariance between Standard Precipitation-Evapotranspiration Index (SPEI) and normalized difference vegetation index and (c) summary coefficients for the protected areas of the spatial autoregressive model performed to evaluate short-term covariance between SPEI and LAI. Values in (b) and (c) are for all forest types. Averages for non-protected areas are indicated by the dashed lines and the error bars represent 99% confidence intervals

is correlated to loss ( $r = 0.87$  for NDVI and  $r = 0.48$  for LAI) and gain ( $r = 0.44$  and  $r = 0.32$  for LAI,  $p < .05$  in both cases) (Figure 10a).

We found that the non-native *Eucalyptus* had low gain-to-loss ratios following droughts (Figure 9b), which explains the decline in leaf area in 26% of examined *Eucalyptus* plots, a significantly higher percentage than the average of 12% (Table S2). Looking at the long-term CCI, we found that growth in most Spanish forests

is similarly impacted by SPEI trends (Figure 10c). Only two groups, *Pinus pinaster* associated with xeric sites, as well as *Quercus robur* and *Quercus petraea*, were more severely pressured by climate change (Figure 10c). Combining this with previous findings, we conclude that the overall greening of Spain is possible in part because of species which are resilient to drought while the decline in many *Eucalyptus* plantations (26%) is mostly caused by their low short-term resilience.

### 3.5 | Resistance of protected areas to climate change and effect of previous land cover

Canopy greenness and leaf area inside protected areas were more stable over the 18-year time-series (Figure 11c). Looking at the covariance between SPEI and canopy greenness results, protected forests were significantly less sensitive to drought than unprotected forests (i.e. lost and gained less greenness during droughts; Figure 11b). On the other hand, the equivalent response in leaf area change was not significant indicating that the leaf area did not change much in these forests (Figure 11c). No significant difference was found in the gain-to-loss ratio in the most extreme droughts yet, since, as mentioned previously, Spanish forest canopy greenness was found to typically resilient (Figure 11a).

Including whether or not forested areas were previous agricultural lands did not improve the fits of any of our models (i.e. changes the AIC were less than 2; Table S1).

## 4 | DISCUSSION

### 4.1 | Long-term and short-term CCI on forest canopy

Regression and breakpoint analyses of the NDVI time-series shed light on why Spanish forest canopies are so remarkably resilient to climate change, greening despite the region becoming drier. The NDVI time-series covaried closely with relative water availability ( $R^2 = .49$ ) which agrees with previous findings (Gouveia et al., 2012). In the short term, this covariance caused significant variation in canopy greenness and leaf area in response to drought events, with average losses in LAI during strong droughts amounting to  $0.32 \text{ m}^2/\text{m}^2$ ; however, in the long term, this covariance had a much smaller influence on greening trends with predicted changes to LAI amounting on average to  $0.0002 \text{ m}^2 \text{ m}^{-2} \text{ year}^{-1}$  with a standard deviation of 0.004. Drought effects on vegetation are commonly defined as multi-scalar phenomenon, progressing from stomatal closure, and/or leaf abscission to embolism and hydraulic failure in response to water deficit (McKee et al, 1993 ; Vicente-Serrano et al., 2010), but few studies on forest resilience have dealt with this temporal aspect of trees response to drought (Camarero et al., 2018; Schwalm et al., 2017). The use of SPEI at different accumulation periods  $X$  allowed us to account for lags in forest response to drought and to better capture the effect of water deficit on vegetation. Recent analyses of Spanish forest indicate that drought was responsible for 50% of damage to forest canopies ('damage' defined as >25% defoliation of the canopy), followed by insects and pathogens that were responsible for 24% of damage (IDF España, 2017). However, these analyses focus on the sensitivity of woodlands not recovery. On average, 80% of losses in greenness were recovered in the 18 months following a drought event, while the remaining 20% were recovered in subsequent years to give the long-term greening trend we observe (Figure 10a,b; Figure S7). These results suggest that forests in Spain

mostly undergo defoliation that is easily recoverable in the wet period following a drought while 20% of the damages that can be more permanent are outgrown in the next couple years before another drought happens. Water availability in period after severe drought is important for forest recovery (Jiang et al., 2019), as we indeed found that greater water availability (maximum SPEI) led to greater recovery while minimum SPEI was associated with bigger losses in greenness and leaf area.

Surprisingly, forests exposed to the strongest droughts had the highest gain-to-loss ratios (Figure 10b). This phenomenon was observed in several other studies on the effect of drought on forest canopy and basal area (Delissio & Primack, 2003; Dorman, Perevolotsky, Sarris, & Svoray, 2015; Gazol et al., 2018—see supplementary material—Schwartz, Budsock, & Uriarte, 2019; Serra-Maluquer, Mencuccini, & Martínez-Vilalta, 2018; Slik, 2004), but remains poorly understood. Perhaps intense droughts have a thinning effect on forests as they are associated with greater losses in leaf area (Figure 9a). These losses in leaf area which represent an increase in forest litterfall as well as canopy openings could reduce stand transpiration, interception of precipitation and competition for light and water resources (Delissio & Primack, 2003; Navarro-Cerrillo et al., 2019; Schwartz et al., 2019; Sohn, Hartig, Kohler, Huss, & Bauhus, 2016). In turn, the reduction of competition aboveground and belowground can boost the recruitment of more resilient trees and the productivity of the surviving trees during the wet period following an intense drought (Schwartz et al., 2019; Slik, 2004). It is possible however that observed increases in remotely sensed short-term resilience are not related to the detected increases in basal area increment (Dorman et al., 2015; Gazol et al., 2018), but instead to the increase in understory photosynthetic activity (Breshears et al., 2005; McDowell et al., 2008; Schwartz et al., 2019).

### 4.2 | Spain is greening despite increased aridity

The impact of climate change on forest health is a highly topical issue (Allen et al., 2010). Temperatures in the region have increased by  $1.3^\circ\text{C}$ , compared to  $0.85^\circ\text{C}$  worldwide, since the end of the 19th century, and rainfall patterns have decreased by 20% in some regions but have increased in others (Barbeta, Ogaya, & Peñuelas, 2013; Guiot & Cramer, 2016b; UNEP/MAP, 2016; Zhu et al., 2016). We found an average decrease in the water balance of  $1.9 \text{ mm/year}$  over our pixels for the period 2000–2017, which follows decreases in precipitation by  $1.9 \text{ mm/year}$  and increases in temperature by  $0.03^\circ\text{C/year}$  for the period 1961–2011 (Vicente-Serrano, Azorin-Molina, et al., 2014). Indeed, several studies have reported localized dieback associated with extreme drought events in Spain (Guada, Camarero, Sánchez-Salguero, & Cerrillo, 2016; Lloret & García, 2016; Lloret, Siscart, & Dalmases, 2004; Molina-Venegas, Llorente-Culebras, Ruiz-Benito, & Rodríguez, 2018; Ogaya et al., 2015).

However, the narrative of declining forest health associated with global warming contrasts with observations made by multispectral

sensors, which indicate that Spain is greening (Domingo et al., 2008; González-Alonso, Cuevas, Calle, Casanova, & Romo, 2004; González-Alonso et al., 2006; Hill, Stellmes, Udelhoven, Röder, & Sommer, 2008; Khorchani et al., 2018; Peñuelas et al., 2002). We found that 75% of Spanish forested pixels analysed had become greener over the past 18 years (+0.03 NDVI and +0.18 m<sup>2</sup> m<sup>-2</sup> year<sup>-1</sup> LAI). Suggested causes of these trends include increased radiation (Khorchani et al., 2018), land use change (García-Ruiz & Lana-Renault, 2011; Khorchani et al., 2018), partly due abandonment of grazing lands in last few decades (Carnicer et al., 2014; Hill et al., 2008) and increased basal area of woodlands that are no longer used for timber or charcoal (Otero et al., 2015). Spain joins many other regions of the world that are greening despite climate change (Eastman et al., 2013; Zhu et al., 2016): these global studies have suggested nitrogen fertilizer application and deposition, CO<sub>2</sub> fertilization and more favourable climate conditions could all contribute to the trend (Eastman et al., 2013; Los, 2013; Mao et al., 2013; Zhu et al., 2016).

### 4.3 | Dense canopies are most sensitive to drought

Changes in satellite-detected greenness are known to be correlated to leaf biomass change and photosynthetic activity (Asrar et al., 1989; Baret & Guyot, 1991; Carlson & Ripley, 1997; Cihlar et al., 1991; Tucker & Sellers, 1986; Zhang et al., 2003), and many studies have used this information to estimate forest biomass from satellite (Galidaki et al., 2017; le Maire et al., 2011). Examining the relation between the Spanish national forest inventory basal area and greenness we found a significant positive relationship which supports these studies. Consequently, our results indicate that in Spain higher canopy density increases competition and transpiration leading to increased sensitivity to drought (i.e. losses in LAI) which agrees with previous studies on forest density effects (Bottero et al., 2017; Navarro-Cerrillo et al., 2019; Raz-Yaseef, Yakir, Schiller, & Cohen, 2012). We found that forests that have denser canopies, that is, have a high average NDVI or LAI, are more sensitive to changes in SPEI. The effect of forest density becomes however insignificant when looking at the gain-to-loss ratio to extreme drought (short-term CGW), meaning that density-caused losses in greenness or leaf area are always followed by similar NDVI or LAI gains. We believe that the lack of forest-density effect on short-term greenness resilience is mostly due to the overall resilience of the forests, and that stronger droughts will cause this effect to be significantly negative.

### 4.4 | Differential response of forest types and protected areas

Spanish forests are currently dominated by pines, which occupy 67% of forested lands, including *P. pinaster* and *P. sylvestris* in big proportions (Figure S2; Brus et al., 2012). The second most dominant species groups are oaks (22% including *Q. robur* and *Q. petraea*),

secondary successional species, which are favoured by managers and are reported to be advancing on pines (Brus et al., 2012; Martín-Alcón et al., 2015; Pausas et al., 2004). Understanding the resilience to drought of these two groups is therefore paramount for Spanish ecosystems. Here, forest types differed in response to droughts, indicating differences in the drought resilience behaviours of species that dominate these forest types (Hwang et al., 2017). We found that *Castanea* lost little greenness during drought, consistent with anisohydric species that keep their stomata open and continue photosynthesizing for longer when droughts occur (Martínez-Sancho, Navas, Seidel, Dorado-Liñán, & Menzel, 2017; Mota et al., 2018). This 'tolerance behaviour' results in their leaf water potential becoming increasingly negative during drought periods, which can push anisohydric trees beyond their limited hydraulic safety margins, leading susceptible species to hydraulic failure, that can be temporary or permanent (Kannenberg et al., 2019; Martínez-Sancho et al., 2017). At the other end of the spectrum, *P. pinaster* lost many leaves in response to drought. Isohydric species, like *P. pinaster*, tend to close their stomata to preserve hydraulic conductivity and then drop leaves as the drought continues (Galiano, Martínez-Vilalta, & Lloret, 2011). Species with an 'avoidance behaviour' can die during prolonged droughts as a result of hydraulic failure. Some studies also suggest that carbon starvation can occur (Galiano et al., 2011; Savi et al., 2019; Sevanto, McDowell, Dickman, Pangle, & Pockman, 2014), but other researchers remain unconvinced that this mechanism is important (Körner, 2013; Muller et al., 2011).

Plantations of *Eucalyptus* responded differently to other forest types, recovering slowly from drought (Figure 10a) and in a number of cases (26%), higher than that of other species (12%), failing to recover (Table S2). There are reports of *Eucalyptus* declining in response to drought in the Mediterranean regions of their native Australia (Brouwers, Matusick, Ruthrof, Lyons, & Hardy, 2013; Matusick et al., 2018; Matusick, Ruthrof, & St Hardy, 2012). In Spain, *Eucalyptus* is planted in wetter regions that have not become drier over the past 18 years, and most reports and studies discuss *Eucalyptus* in the context of timber production, pests and diseases (Queirós et al., 2020; IDF España, 2017) rather than their response to drought (Barradas et al., 2018; Peñuelas, Lloret, & Montoya, 2001).

The study provides no evidence of widespread permanent hydraulic failure of either isohydric or anisohydric species, as most canopies we investigated recovered in greenness following drought events. With the exception of *Eucalyptus* plantations, there were no significant differences in the gain-to-loss ratio of forest types, which might indicate that these contrasting behaviours were similarly effective in terms of canopy resilience. These findings need to be treated with caution, given that few of the forest types were comprised of single species. For instance, *P. sylvestris* is recognized as an isohydric species (Galiano et al., 2011), but forest classified as dominated by this species did not respond to drought in the way expected of an isohydric species—they lost about average canopy greenness during drought (Figure 11a)—so we suspect that other woody species contributed to the greenness signal. Additionally, stands with medium-low canopy cover that leave

exposed understorey and shrub or herbaceous which can contribute to the greenness. Focusing analyses on stands with known species composition will help clarify the responses of species and communities to drought (e.g. Hwang et al., 2017). Furthermore, studies that link canopy greenness trends with detailed physiological measurements are needed to understand the mechanistic explanations behind resilience.

Our regression analyses demonstrate that managements of woodlands in protected areas have made their canopy greenness, that is, NDVI, more resilient to drought because their short-term responsiveness to water availability is relatively low (Figure 11b). When looking at LAI, however, the response to water availability was not significantly different in protected areas, contradicting the NDVI results (Figure 11c). To extract more information on the matter, we decided to look at the number of declining LAI pixels instead of the effect on all pixels; it was significantly smaller in Natura 2000 forests and the decline was also significantly less pronounced (Table S2). These results indicate that Natura 2000 ZEC might have a more positive effect on the forest canopy resilience. Field studies in the region have demonstrated that thinning can improve resilience (Navarro-Cerrillo et al., 2019) but thinning can also decrease leaf area. This is the first study to determine the effect of these protective measures on forest canopy resilience to climate change at the national scale from satellite imagery. More studies are needed to determine which measures in these protected areas are actually enhancing forest resilience. As mentioned in Section 2.2, the management of Natura 2000 sites varies greatly depending on the responsible administration, the funds available, the biogeographic region and whether or not the site is a Nationally Designated Protected area, therefore, future studies can take these factors into account to uncover more information on management effectiveness. Finally, gain-to-loss ratios obtained by breakpoint analysis, as well as LAI response, could be failing to show that protected forests are more resilient to drought mainly because of the overall resilience of Spanish forest canopy greenness to past changes in water availability. Alternatively, given that the short-term NDVI responsiveness to drought was not very strong, it could be that protected areas have failed to make a difference in forest resilience thus far; more data are needed to evaluate this. As mentioned in van der Plas et al. (2018), many protected areas have been established recently; thus, there has been insufficient time for the implementation of their transformative management actions. In addition, many have been created to protect and restore degraded and abandoned lands which require extra time to recover (van der Plas et al., 2018). Although we found no effect of land-cover change from 1990 to 2000 on the resilience of forest canopies, we did not evaluate the effect of past forest management, which would also be interesting to study.

#### 4.5 | Research and management implications

Returning to the questions posed at the beginning of this study, it is now possible to state that canopy greenness of Spanish forests have

been remarkably resilient to droughts in the 2000–2017 period: these secondary forests are continuing to accumulate biomass and becoming greener despite climate change making this region hotter and drier. Unlike our expectations, most forest types, regardless of their drought resistance behaviour and management, recovered from losses incurred by extreme drought events. Finally, we demonstrate that protection and management of these forested lands has the potential to be effective in alleviating the effects of climate change on canopies by increasing the forest capacity to resist during a drought.

Breakpoint and regression approaches provide complementary insights into resilience and its components. Short-term covariance between water availability and NDVI or LAI was highly correlated with sensitivity and to a lesser extent recovery measures and could be used to assess the stability of a forest in face climate variation, as well as provide insights into the prevailing drought resistance mechanism of a species. The long-term CCI, on the other hand, can be used to estimate drought pressure on these forests. Finally, breakpoint analysis, which allows losses and recovery of canopy greenness due to drought events to be determined, could be used alongside forest die-off information to determine the tipping point of forests.

Our study has focused on the resilience of forest canopies to drought but shifts in species distribution and changing disturbance regimes will also influence resilience as the climate warms. Several studies have already analysed past shifts in species distribution as well as modelled and predicted future changes in plant communities and their distributions using ground data (García-Valdés, Zavala, Araújo, & Purves, 2013; Lines, 2012; Lloret, Martínez-Vilalta, Serra-Díaz, & Ninyerola, 2013; Rabasa et al., 2013; Ruiz-Labourdette, Nogués-Bravo, Ollero, Schmitz, & Pineda, 2012; Valladares et al., 2014). Most of these studies mentioned a decrease in the climatic suitability in the future for most species and predicted altitudinal shifts. A few mentioned an increase in habitat for broadleaves at the expense of pines while one study predicted an increase in the range of low altitude pines.

Furthermore, extreme drought events increase the risks of fires and insect outbreaks (Allen et al., 2010). Our methodology can be applied to such secondary events if data such as fire occurrence, insect distribution and physiology, and geology is available; and it would be the next natural step to identify management options that would maximize the resilience of forest to different extreme biotic and abiotic events. For instance, fire occurrence data can be tracked from satellite (Justice et al., 2002; Turco, Herrera, Tourigny, Chuvieco, & Provenzale, 2019), and pathogen damage can be detected from hyperspectral data, lidar data or both (Lin, Huang, Wang, Huang, & Liu, 2019; Stereńczak et al., 2019). Furthermore, species composition and stand development information are becoming more and more accessible thanks to hyperspectral imagery and repeat lidar scans (Coomes et al. 2017; Jucker et al., 2018; Nunes, Davey, & Coomes, 2017; Simonson, Allen, & Coomes, 2012; Simonson, Ruiz-Benito, Valladares, & Coomes, 2016). Future work could also explore whether stand

height, age, soil type and species composition influence resilience; and include field data at the same resolution to gain a better understanding of the linkages between remotely sensed greenness and forest change.

## ACKNOWLEDGEMENTS

S.K. is supported by Cambridge Commonwealth, European & International Trust. We acknowledge MAPA (Ministerio de Agricultura, Pesca y Alimentación) for the access to the Spanish National Forest Inventory. We thank Dr. Paloma Ruiz-Benito for helping us access the Spanish National Inventory data, Dr. Tom Swinfield and Dr. Javier Igea for their advice on spatial auto-correlation models, Dr. Thiago Burghi for his advice on modelling, and Miss Eleanor Hammond for reviewing the manuscript. Finally, we would like to thank the anonymous reviewers for the valuable comments and suggestions which helped us improve the manuscript.

## DATA AVAILABILITY STATEMENT

Data used in this study are publicly available at Figshare (<https://doi.org/10.6084/m9.figshare.12612416>). Code used to produce these results is available upon request from the authors.

## ORCID

Sacha Khoury  <https://orcid.org/0000-0002-1980-5365>

David A. Coomes  <https://orcid.org/0000-0002-8261-2582>

## REFERENCES

- Allen, C. D., Macalady, A. K., Chenchouni, H., Bachelet, D., McDowell, N., Vennetier, M., ... Cobb, N. (2010). A global overview of drought and heat-induced tree mortality reveals emerging climate change risks for forests. *Forest Ecology and Management*, 259(4), 660–684. <https://doi.org/10.1016/j.foreco.2009.09.001>
- Anderegg, W. R. L., Schwalm, C., Biondi, F., Camarero, J. J., Koch, G., Litvak, M., ... Pacala, S. (2015). Pervasive drought legacies in forest ecosystems and their implications for carbon cycle models. *Science*, 349(6247), 528–532. <https://doi.org/10.1126/science.aab1833>
- Asrar, G., Myneni, R. B., & Kanemasu, E. T. (1989). Estimation of plant canopy attributes from spectral reflectance measurements. In G. Asrar (Ed.), *Theory and applications of optical remote sensing* (pp. 252–296). New York: Wiley. Retrieved from [https://books.google.co.uk/books/about/Theory\\_and\\_Applications\\_of\\_Optical\\_Remot.html?id=9gRPA AAAMAAJ&redir\\_esc=y](https://books.google.co.uk/books/about/Theory_and_Applications_of_Optical_Remot.html?id=9gRPA AAAMAAJ&redir_esc=y)
- Azarin-Molina, C., Vicente-Serrano, S. M., McVicar, T. R., Jerez, S., Sanchez-Lorenzo, A., López-Moreno, J.-I., ... Espirito-Santo, F. (2014). Homogenization and assessment of observed near-surface wind speed trends over Spain and Portugal, 1961–2011. *Journal of Climate*, 27(10), 3692–3712. <https://doi.org/10.1175/JCLI-D-13-00652.1>
- Barbeta, A., Ogaya, R., & Peñuelas, J. (2013). Dampening effects of long-term experimental drought on growth and mortality rates of a Holm oak forest. *Global Change Biology*, 19(10), 3133–3144. <https://doi.org/10.1111/gcb.12269>
- Baret, F., & Guyot, G. (1991). Potentials and limits of vegetation indices for LAI and APAR assessment. *Remote Sensing of Environment*, 35(2–3), 161–173. [https://doi.org/10.1016/0034-4257\(91\)90009-U](https://doi.org/10.1016/0034-4257(91)90009-U)
- Barradas, C., Pinto, G., Correia, B., Castro, B. B., Phillips, A. J. L., & Alves, A. (2018). Drought × disease interaction in *Eucalyptus globulus* under *Neofusicoccum eucalyptorum* infection. *Plant Pathology*, 67(1), 87–96. <https://doi.org/10.1111/ppa.12703>
- Baskerville, G. L. (1972). Use of logarithmic regression in the estimation of plant biomass. *Canadian Journal of Forest Research*, 2(1), 49–53. <https://doi.org/10.1139/x72-009>
- Beguieria, S., & Vicente-Serrano, S. M. (2017). SPEI: Calculation of the standardised precipitation-evapotranspiration index. R Package Version, 1.7. <https://doi.org/10.1175/2009JCLI2909.1>. Retrieved from <http://sac.csic.es/spei/>
- Beguieria, S., Vicente-Serrano, S. M., Reig, F., & Latorre, B. (2014). Standardized precipitation evapotranspiration index (SPEI) revisited: Parameter fitting, evapotranspiration models, tools, datasets and drought monitoring. *International Journal of Climatology*, 34(10), 3001–3023. <https://doi.org/10.1002/joc.3887>
- Bivand, R., & Piras, G. (2019). spatialreg: Spatial regression analysis. R package version 1.1-3. Retrieved from <https://r-spatial.github.io/spatialreg/>
- Bottero, A., D'Amato, A. W., Palik, B. J., Bradford, J. B., Fraver, S., Battaglia, M. A., & Asherin, L. A. (2017). Density-dependent vulnerability of forest ecosystems to drought. *Journal of Applied Ecology*, 54(6), 1605–1614. <https://doi.org/10.1111/1365-2664.12847>
- Breshears, D. D., Cobb, N. S., Rich, P. M., Price, K. P., Allen, C. D., Balice, R. G., ... Meyer, C. W. (2005). Regional vegetation die-off in response to global-change-type drought. *Proceedings of the National Academy of Sciences of the United States of America*, 102(42), 15144–15148. <https://doi.org/10.1073/pnas.0505734102>
- Brouwers, N., Matusick, G., Ruthrof, K., Lyons, T., & Hardy, G. (2013). Landscape-scale assessment of tree crown dieback following extreme drought and heat in a Mediterranean eucalypt forest ecosystem. *Landscape Ecology*, 28(1), 69–80. <https://doi.org/10.1007/s10980-012-9815-3>
- Brus, D. J., Hengeveld, G. M., Walvoort, D. J. J., Goedhart, P. W., Heidema, A. H., Nabuurs, G. J., & Gunia, K. (2012). Statistical mapping of tree species over Europe. *European Journal of Forest Research*, 131(1), 145–157. <https://doi.org/10.1007/s10342-011-0513-5>
- Camarero, J. J., Gazol, A., Sangüesa-Barreda, G., Cantero, A., Sánchez-Salguero, R., Sánchez-Miranda, A., ... Ibáñez, R. (2018). Forest growth responses to drought at short- and long-term scales in Spain: Squeezing the stress memory from tree rings. *Frontiers in Ecology and Evolution*, 6, 9. <https://doi.org/10.3389/fevo.2018.00009>
- Carlson, T. N., & Ripley, D. A. (1977). On the relation between NDVI, fractional vegetation cover, and leaf area index. *Remote Sensing of Environment*, 62(3), 241–252. [https://doi.org/10.1016/S0034-4257\(97\)00104-1](https://doi.org/10.1016/S0034-4257(97)00104-1)
- Carnicer, J., Barbeta, A., Sperlich, D., Coll, M., & Peñuelas, J. (2013). Contrasting trait syndromes in angiosperms and conifers are associated with different responses of tree growth to temperature on a large scale. *Frontiers in Plant Science*, 4, 409. <https://doi.org/10.3389/fpls.2013.00409>
- Carnicer, J., Coll, M., Ninyerola, M., Pons, X., Sánchez, G., & Peñuelas, J. (2011). Widespread crown condition decline, food web disruption, and amplified tree mortality with increased climate change-type drought. *Proceedings of the National Academy of Sciences of the United States of America*, 108(4), 1474–1478. <https://doi.org/10.1073/pnas.1010070108>
- Carnicer, J., Coll, M., Pons, X., Ninyerola, M., Vayreda, J., & Peñuelas, J. (2014). Large-scale recruitment limitation in Mediterranean pines: The role of *Quercus ilex* and forest successional advance as key regional drivers. *Global Ecology and Biogeography*, 23(3), 371–384. <https://doi.org/10.1111/geb.12111>
- Cihlar, J., St-Laurent, L., & Dyer, J. A. (1991). Relation between the normalized difference vegetation index and ecological variables. *Remote Sensing of Environment*, 35(2–3), 279–298. [https://doi.org/10.1016/0034-4257\(91\)90018-2](https://doi.org/10.1016/0034-4257(91)90018-2)
- Coomes, D. A., Dalponte, M., Jucker, T., Asner, G. P., Banin, L. F., Burslem, D. F. R. P., ... Qie, L. (2017). Area-based vs tree-centric approaches to

- mapping forest carbon in Southeast Asian forests from airborne laser scanning data. *Remote Sensing of Environment*, 194, 77–88. <https://doi.org/10.1016/j.rse.2017.03.017>
- Coops, N. C., Johnson, M., Wulder, M. A., & White, J. C. (2006). Assessment of QuickBird high spatial resolution imagery to detect red attack damage due to mountain pine beetle infestation. *Remote Sensing of Environment*, 103(1), 67–80. <https://doi.org/10.1016/j.rse.2006.03.012>
- Dakos, V., Carpenter, S. R., van Nes, E. H., & Scheffer, M. (2015). Resilience indicators: Prospects and limitations for early warnings of regime shifts. *Philosophical Transactions of the Royal Society B: Biological Sciences*, 370(1659), 20130263. <https://doi.org/10.1098/rstb.2013.0263>
- de la Guerra, M. M., Martínez Alandi, C., Atauri Mezquida, J. A., Gómez-Limón García, J., Puertas Blázquez, J., & García Ventura, D. (2017). *EUROPARC-España. 2017 Anuario 2016 del estado de las áreas protegidas en España*. In F. I. Para Los Espacios & N. Fernando González Bernáldez (Eds.). Madrid: Fundación Interuniversitaria Fernando González Bernáldez para los espacios naturales.
- De Oliveira Silveira, E. M., De Carvalho, L. M. T., Acerbi, F. W., & De Mello, J. M. (2008). The assessment of vegetation seasonal dynamics using multitemporal NDVI and EVI images derived from MODIS. *Cerne*, 14(2), 177–184. <https://doi.org/10.1109/MULTI TEMP.2007.4293049>
- Delissio, L. J., & Primack, R. B. (2003). The impact of drought on the population dynamics of canopy-tree seedlings in an aseasonal Malaysian rain forest. *Journal of Tropical Ecology*, 19(05), 489–500. <https://doi.org/10.1017/S0266467403003547>
- Didan, K. (2015a). MOD13Q1 MODIS/terra vegetation indices 16-day L3 global 250m SIN grid V006 [Data set]. NASA EOSDIS LP DAAC. <https://doi.org/10.5067/MODIS/MOD13Q1.006>
- Didan, K. (2015b). MYD13Q1 MODIS/aqua vegetation indices 16-day L3 global 250m SIN grid V006 [Data set]. NASA EOSDIS LP DAAC. <https://doi.org/10.5067/MODIS/MYD13Q1.006>
- Domingo, A. S., Javier, C., Paruelo Jose, M., & Miguel, D. (2008). Trends in the surface vegetation dynamics of the national parks of Spain as observed by satellite sensors. *Applied Vegetation Science*, 11(4), 431–440. <https://doi.org/10.3170/2008-7-18522>
- Dorman, M., Perevolotsky, A., Sarris, D., & Svoray, T. (2015). The effect of rainfall and competition intensity on forest response to drought: Lessons learned from a dry extreme. *Oecologia*, 177(4), 1025–1038. <https://doi.org/10.1007/s00442-015-3229-2>
- Eastman, J., Sangermano, F., Machado, E., Rogan, J., Anyamba, A., Eastman, J. R., ... Anyamba, A. (2013). Global trends in seasonality of normalized difference vegetation index (NDVI), 1982–2011. *Remote Sensing*, 5(10), 4799–4818. <https://doi.org/10.3390/rs5104799>
- Evrendilek, F., & Gulbeyaz, O. (2008). Deriving vegetation dynamics of natural terrestrial ecosystems from MODIS NDVI/EVI data over Turkey. *Sensors*, 8(9), 5270–5302. <https://doi.org/10.3390/s8095270>
- Fao & Plan Bleu. (2013). State of Mediterranean Forests (SoMF). Concept Paper.
- Folke, C., Carpenter, S. R., Walker, B., Scheffer, M., Chapin, T., & Rockström, J. (2010). Resilience thinking: Integrating resilience, adaptability and transformability. *Ecology and Society*, 15(4), 20. <https://doi.org/10.5751/ES-03610-150420>
- Fraser, R. H., & Latifovic, R. (2005). Mapping insect-induced tree defoliation and mortality using coarse spatial resolution satellite imagery. *International Journal of Remote Sensing*, 26(1), 193–200. <https://doi.org/10.1080/01431160410001716923>
- Galiano, L., Martínez-Vilalta, J., & Lloret, F. (2011). Carbon reserves and canopy defoliation determine the recovery of Scots pine 4 yr after a drought episode. *New Phytologist*, 190(3), 750–759. <https://doi.org/10.1111/j.1469-8137.2010.03628.x>
- Galidaki, G., Zianis, D., Gitas, I., Radoglou, K., Karathanassi, V., Tsakiri-Strati, M., ... Mallinis, G. (2017). Vegetation biomass estimation with remote sensing: focus on forest and other wooded land over the Mediterranean ecosystem. *International Journal of Remote Sensing*, 38(7), 1940–1966. <https://doi.org/10.1080/01431161.2016.1266113>
- Garrity, S. R., Allen, C. D., Brumby, S. P., Gangodagamage, C., McDowell, N. G., & Cai, D. M. (2013). Quantifying tree mortality in a mixed species woodland using multitemporal high spatial resolution satellite imagery. *Remote Sensing of Environment*, 129, 54–65. <https://doi.org/10.1016/j.rse.2012.10.029>
- García-Ruiz, J. M., & Lana-Renault, N. (2011). Hydrological and erosive consequences of farmland abandonment in Europe, with special reference to the Mediterranean region – A review. *Agriculture, Ecosystems and Environment*, 140(3–4), 317–338. <https://doi.org/10.1016/j.agee.2011.01.003>
- García-Valdés, R., Zavala, M. A., Araújo, M. B., & Purves, D. W. (2013). Chasing a moving target: Projecting climate change-induced shifts in non-equilibrium tree species distributions. *Journal of Ecology*, 101(2), 441–453. <https://doi.org/10.1111/1365-2745.12049>
- Gavinet, J., Prévosto, B., & Fernandez, C. (2016). Introducing resprouters to enhance Mediterranean forest resilience: Importance of functional traits to select species according to a gradient of pine density. *Journal of Applied Ecology*, 53(6), 1735–1745. <https://doi.org/10.1111/1365-2664.12716>
- Gazol, A., Camarero, J. J., Vicente-Serrano, S. M., Sánchez-Salguero, R., Gutiérrez, E., de Luis, M., ... Galván, J. D. (2018). Forest resilience to drought varies across biomes. *Global Change Biology*, 24(5), 2143–2158. <https://doi.org/10.1111/gcb.14082>
- Gómez-González, S., Ojeda, F., & Fernandes, P. M. (2018). Portugal and Chile: Longing for sustainable forestry while rising from the ashes. *Environmental Science & Policy*, 81, 104–107. <https://doi.org/10.1016/J.ENVSCI.2017.11.006>
- González-Alonso, F., Cuevas, J. M., Calle, A., Casanova, J. L., & Romo, A. (2004). Spanish vegetation monitoring during the period 1987–2001 using NOAA-AVHRR images. *International Journal of Remote Sensing*, 25(1), 3–6. <https://doi.org/10.1080/0143116031000115229>
- González-Alonso, F., Merino-De-Miguel, S., Roldán-Zamarrón, A., García-Gigorro, S., & Cuevas, J. M. (2006). Forest biomass estimation through NDVI composites. The role of remotely sensed data to assess Spanish forests as carbon sinks. *International Journal of Remote Sensing*, 27(24), 5409–5415. <https://doi.org/10.1080/01431160600830748>
- Gouveia, C. M., Bastos, A., Trigo, R. M., & Dacamara, C. C. (2012). Drought impacts on vegetation in the pre- and post-fire events over Iberian Peninsula. *Natural Hazards and Earth System Science*, 12(10), 3123–3137. <https://doi.org/10.5194/nhess-12-3123-2012>
- Guada, G., Camarero, J. J., Sánchez-Salguero, R., & Cerrillo, R. M. N. (2016). Limited growth recovery after drought-induced forest die-back in very defoliated trees of two pine species. *Frontiers in Plant Science*, 7, 418. <https://doi.org/10.3389/fpls.2016.00418>
- Guiot, J., & Cramer, W. (2016a). Climate change: The 2015 Paris Agreement thresholds and Mediterranean basin ecosystems. *Science*, 354(6311), 4528–4532.
- Guiot, J., & Cramer, W. (2016b). Climate change, the Paris Agreement thresholds and Mediterranean ecosystems. *Science*, 354(6311), 465–468. <https://doi.org/10.1126/science.aah5015>
- Hart, S. J., & Veblen, T. T. (2015). Detection of spruce beetle-induced tree mortality using high- and medium-resolution remotely sensed imagery. *Remote Sensing of Environment*, 168, 134–145. <https://doi.org/10.1016/j.rse.2015.06.015>
- Hill, J., Stellmes, M., Udelhoven, T., Röder, A., & Sommer, S. (2008). Mediterranean desertification and land degradation: Mapping related land use change syndromes based on satellite observations. *Global and Planetary Change*, 64(3–4), 146–157. <https://doi.org/10.1016/J.GLOPLACHA.2008.10.005>
- Hodgson, D., McDonald, J. L., & Hosken, D. J. (2015). Feature issue: Some thoughts on resilience what do you mean, “resilient”? *Trends*

- in *Ecology & Evolution*, 30(9), 503–506. <https://doi.org/10.1016/j.tree.2015.06.010>
- Hwang, T., Gholizadeh, H., Sims, D. A., Novick, K. A., Brzostek, E. R., Phillips, R. P., ... Rahman, A. F. (2017). Capturing species-level drought responses in a temperate deciduous forest using ratios of photochemical reflectance indices between sunlit and shaded canopies. *Remote Sensing of Environment*, 199(August), 350–359. <https://doi.org/10.1016/j.rse.2017.07.033>
- IDF España. (2017). *Inventario de daños forestales (IDF) en España. Red europea de Seguimiento de daños en los bosques (Red de Nivel I)*. Madrid, Spain: Resultados del Muestreo de 2017. [https://www.mapa.gob.es/es/desarrollo-rural/temas/politica-forestal/inventariodedanosforrestales2017\\_tcm30-441605.pdf](https://www.mapa.gob.es/es/desarrollo-rural/temas/politica-forestal/inventariodedanosforrestales2017_tcm30-441605.pdf)
- Jamali, S., Jönsson, P., Eklundh, L., Ardö, J., & Seaquist, J. (2015). Detecting changes in vegetation trends using time series segmentation. *Remote Sensing of Environment*, 156, 182–195. <https://doi.org/10.1016/j.rse.2014.09.010>
- Jamali, S., & Tomov, H. (2017). DBEST: Detecting breakpoints and estimating segments in trend. CRAN. R Package Version 1.8. Retrieved from <https://rdr.io/cran/DBEST/>
- Jarvis, A., Reuter, H. I., Nelson, A., & Guevara, E. (2008). Hole-filled SRTM for the globe Version 4, available from the CGIAR-CSI SRTM 90m Database. Retrieved from <http://srtm.csi.cgiar.org>
- Jiang, P., Liu, H., Piao, S., Ciais, P., Wu, X., Yin, Y., & Wang, H. (2019). Enhanced growth after extreme wetness compensates for post-drought carbon loss in dry forests. *Nature Communications*, 10(1), 195. <https://doi.org/10.1038/s41467-018-08229-z>
- Jucker, T., Asner, G. P., Dalponte, M., Brodrick, P. G., Philipson, C. D., Vaughn, N. R., ... Coomes, D. A. (2018). Estimating aboveground carbon density and its uncertainty in Borneo's structurally complex tropical forests using airborne laser scanning. *Biogeosciences*, 15, 3811–3830. <https://doi.org/10.5194/bg-15-3811-2018>
- Justice, C. O., Giglio, L., Korontzi, S., Owens, J., Morisette, J. T., Roy, D., ... Kaufman, Y. (2002). The MODIS fire products. *Remote Sensing of Environment*, 83(1–2), 244–262. [https://doi.org/10.1016/S0034-4257\(02\)00076-7](https://doi.org/10.1016/S0034-4257(02)00076-7)
- Kannenbergh, S. A., Novick, K. A., Alexander, M. R., Maxwell, J. T., Moore, D. J. P., Phillips, R. P., & Anderegg, W. R. L. (2019). Linking drought legacy effects across scales: From leaves to tree rings to ecosystems. *Global Change Biology*, 25(9), 2978–2992. <https://doi.org/10.1111/gcb.14710>
- Khorchani, M., Vicente-Serrano, S. M., Azorin-Molina, C., Garcia, M., Martín-Hernandez, N., Peña-Gallardo, M., ... Domínguez-Castro, F. (2018). Trends in LST over the peninsular Spain as derived from the AVHRR imagery data. *Global and Planetary Change*, 166, 75–93. <https://doi.org/10.1016/j.gloplacha.2018.04.006>
- Körner, C. (2013). Growth controls photosynthesis - mostly. *Nova Acta Leopoldina*. N.F., 114, 273–283. <https://www.researchgate.net/publication/236680450>
- le Maire, G., Francois, C., Soudani, K., Davi, H., Le Dantec, V., Saugier, B., & Dufrene, E. (2006). Forest leaf area index determination: A multi-year satellite-independent method based on within-stand normalized difference vegetation index spatial variability. *Journal of Geophysical Research*, 111, G02027. <https://doi.org/10.1029/2005JG000122>
- le Maire, G., Marsden, C., Nouvellon, Y., Grinand, C., Hakamada, R., Stape, J., & Laclau, J.-P. (2011). MODIS NDVI time-series allow the monitoring of Eucalyptus plantation biomass. *Remote Sensing of Environment*, 115(10), 2613–2625. <https://doi.org/10.1016/j.rse.2011.05.017>
- Lin, Q., Huang, H., Wang, J., Huang, K., & Liu, Y. (2019). Detection of Pine Shoot Beetle (PSB) stress on pine forests at individual tree level using UAV-based hyperspectral imagery and Lidar. *Remote Sensing*, 11(21), 2540. <https://doi.org/10.3390/rs11212540>
- Lines, E. (2012). *Forest dynamics at regional scales: Predictive models constrained with inventory data*. PhD thesis, University of Cambridge. Retrieved from <http://www.dspace.cam.ac.uk/handle/1810/243636>
- Lloret, F., & García, C. (2016). Inbreeding and neighbouring vegetation drive drought-induced die-off within juniper populations. *Functional Ecology*, 30(10), 1696–1704. <https://doi.org/10.1111/1365-2435.12655>
- Lloret, F., Martínez-Vilalta, J., Serra-Díaz, J. M., & Ninyerola, M. (2013). Relationship between projected changes in future climatic suitability and demographic and functional traits of forest tree species in Spain. *Climatic Change*, 120(1–2), 449–462. <https://doi.org/10.1007/s10584-013-0820-6>
- Lloret, F., Siscart, D., & Dalmases, C. (2004). Canopy recovery after drought dieback in holm-oak Mediterranean forests of Catalonia (NE Spain). *Global Change Biology*, 10(12), 2092–2099. <https://doi.org/10.1111/j.1365-2486.2004.00870.x>
- Los, S. O. (2013). Analysis of trends in fused AVHRR and MODIS NDVI data for 1982–2006: Indication for a CO<sub>2</sub> fertilization effect in global vegetation. *Global Biogeochemical Cycles*, 27(2), 318–330. <https://doi.org/10.1002/gbc.20027>
- Machar, I., Vlckova, V., Bucek, A., Vozenilek, V., Salek, L., Jerabkova, L., ... Jerabkova, L. (2017). Modelling of climate conditions in forest vegetation zones as a support tool for forest management strategy in European beech dominated forests. *Forests*, 8(3), 82. <https://doi.org/10.3390/f8030082>
- Mao, J., Shi, X., Thornton, P., Hoffman, F., Zhu, Z., & Myneni, R. (2013). Global latitudinal-asymmetric vegetation growth trends and their driving mechanisms: 1982–2009. *Remote Sensing*, 5(3), 1484–1497. <https://doi.org/10.3390/rs5031484>
- Martín-Alcón, S., Coll, L., & Salekin, S. (2015). Stand-level drivers of tree-species diversification in Mediterranean pine forests after abandonment of traditional practices. *Forest Ecology and Management*, 353, 107–117. <https://doi.org/10.1016/j.foreco.2015.05.022>
- Martínez-Fernández, J., Ruiz-Benito, P., & Zavala, M. A. (2015). Recent land cover changes in Spain across biogeographical regions and protection levels: Implications for conservation policies. *Land Use Policy*, 44, 62–75. <https://doi.org/10.1016/j.landusepol.2014.11.021>
- Martínez-Sancho, E., Navas, L. K. V., Seidel, H., Dorado-Liñán, I., & Menzel, A. (2017). Responses of contrasting tree functional types to air warming and drought. *Forests*, 8(11). <https://doi.org/10.3390/f8110450>
- Matusick, G., Ruthrof, K. X., Kala, J., Brouwers, N. C., Breshears, D. D., & Hardy, G. E. S. J. (2018). Chronic historical drought legacy exacerbates tree mortality and crown dieback during acute heatwave-compounded drought. *Environmental Research Letters*, 13(9), 095002. <https://doi.org/10.1088/1748-9326/aad8cb>
- Matusick, G., Ruthrof, K. X., & St Hardy, G. J. (2012). Drought and heat triggers sudden and severe dieback in a dominant Mediterranean-type woodland species. *Open Journal of Forestry*, 2(4), 183–186. <https://doi.org/10.4236/ojf.2012.24022>
- McDowell, N., Pockman, W. T., Allen, C. D., Breshears, D. D., Cobb, N., Kolb, T., ... Yepez, E. A. (2008). Mechanisms of plant survival and mortality during drought: Why do some plants survive while others succumb to drought? *New Phytologist*, 178(4), 719–739. <https://doi.org/10.1111/j.1469-8137.2008.02436.x>
- McKee, T. B., Doesken, N. J., & Kleist, J. (1993). The relationship of drought frequency and duration to time scales. *Proceedings of the Eighth Conference on Applied Climatology, American Meteorological Society*, 17(22), 179–183. Retrieved from <https://www.semanticscholar.org/paper/THE-RELATIONSHIP-OF-DROUGHT-FREQUENCY-AND-DURATION-McKee-Doesken/c3f7136d6cb726b295eb34565a8270177c57f40f>
- Mochida, K., Saisho, D., & Hirayama, T. (2015). Crop improvement using life cycle datasets acquired under field conditions. *Frontiers in Plant Science*, 6(September), 1–8. <https://doi.org/10.3389/fpls.2015.00740>
- Molina-Venegas, R., Llorente-Culebras, S., Ruiz-Benito, P., & Rodríguez, M. A. (2018). Evolutionary history predicts the response of tree species to forest loss: A case study in peninsular Spain. *PLoS One*, 13(9), e0204365. <https://doi.org/10.1371/journal.pone.0204365>

- Mota, M., Marques, T., Pinto, T., Raimundo, F., Borges, A., Caço, J., & Gomes-Laranjo, J. (2018). Relating plant and soil water content to encourage smart watering in chestnut trees. *Agricultural Water Management*, 203(February), 30–36. <https://doi.org/10.1016/j.agwat.2018.02.002>
- Muller, B., Pantin, F., Génard, M., Turc, O., Freixes, S., Piques, M., & Gibon, Y. (2011). Water deficits uncouple growth from photosynthesis, increase C content, and modify the relationships between C and growth in sink organs. *Journal of Experimental Botany*, 62(6), 1715–1729. <https://doi.org/10.1093/jxb/erq438>
- Myneni, R., Knyazikhin, Y., & Park, T. (2015). MCD15A3H MODIS/Terra+Aqua Leaf Area Index/FPAR 4-day L4 Global 500m SIN Grid V006 [Data set]. NASA EOSDIS Land Processes DAAC. <https://doi.org/10.5067/MODIS/MCD15A3H.006>
- Navarro-Cerrillo, R. M., Sánchez-Salguero, R., Rodriguez, C., Duque Lazo, J., Moreno-Rojas, J. M., Palacios-Rodriguez, G., & Camarero, J. J. (2019). Is thinning an alternative when trees could die in response to drought? The case of planted *Pinus nigra* and *P. sylvestris* stands in southern Spain. *Forest Ecology and Management*, 433, 313–324. <https://doi.org/10.1016/J.FORECO.2018.11.006>
- Nimmo, D. G., Mac Nally, R., Cunningham, S. C., Haslem, A., & Bennett, A. F. (2015). Vive la résistance: Reviving resistance for 21st century conservation. *Trends in Ecology & Evolution*, 30(9), 516–523. <https://doi.org/10.1016/J.TREE.2015.07.008>
- Nunes, M. H., Davey, M. P., & Coomes, D. A. (2017). On the challenges of using field spectroscopy to measure the impact of soil type on leaf traits. *Biogeosciences*, 14(13), 3371–3385. <https://doi.org/10.5194/bg-14-3371-2017>
- Ogaya, R., Barbeta, A., Bañnou, C., & Peñuelas, J. (2015). Satellite data as indicators of tree biomass growth and forest dieback in a Mediterranean holm oak forest. *Annals of Forest Science*, 72(1), 135–144. <https://doi.org/10.1007/s13595-014-0408-y>
- Oliver, T. H., Heard, M. S., Isaac, N. J. B., Roy, D. B., Procter, D., Eigenbrod, F., ... Bullock, J. M. (2015). Biodiversity and resilience of ecosystem functions. *Trends in Ecology & Evolution*, 30(11), 673–684. <https://doi.org/10.1016/j.tree.2015.08.009>
- Otero, I., Marull, J., Tello, E., Diana, G. L., Pons, M., & Coll, F. (2015). Land abandonment, landscape, and biodiversity: Questioning the restorative character of the forest transition in the Mediterranean. *Ecology & Society*, 20(2). <https://doi.org/10.5751/ES-07378-200207>
- Pausas, J. G., Bladé, C., Valdecantos, A., Seva, J. P., Fuentes, D., Alloza, J. A., ... Vallejo, R. (2004). Pines and oaks in the restoration of Mediterranean landscapes of Spain: New perspectives for an old practice – A review. *Plant Ecology*, 171(1/2), 209–220. <https://doi.org/10.1023/b:vege.0000029381.63336.20>
- Peltier, D. M. P., Fell, M., & Ogle, K. (2016). Legacy effects of drought in the southwestern United States: A multi-species synthesis. *Ecological Monographs*, 86(3), 312–326. <https://doi.org/10.1002/ecm.1219>
- Peñuelas, J., Filella, I., & Comas, P. (2002). Changed plant and animal life cycles from 1952 to 2000 in the Mediterranean region. *Global Change Biology*, 8(6), 531–544. <https://doi.org/10.1046/j.1365-2486.2002.00489.x>
- Peñuelas, J., Lloret, F., & Montoya, R. (2001). Severe drought effects on Mediterranean woody flora in Spain. *Forest Science*, 47(2), 214–218.
- Peñuelas, J., Sardans, J., Filella, I., Estiarte, M., Llusà, J., Ogaya, R., ... Terradas, J. (2017). Impacts of global change on Mediterranean forests and their services. *Forests*, 8(12), 1–37. <https://doi.org/10.3390/f8120463>
- Plas, F., Ratcliffe, S., Ruiz-Benito, P., Scherer-Lorenzen, M., Verheyen, K., Wirth, C., ... Allan, E. (2018). Continental mapping of forest ecosystem functions reveals a high but unrealised potential for forest multifunctionality. *Ecology Letters*, 21(1), 31–42. <https://doi.org/10.1111/ele.12868>
- Queirós, L., Deus, E., Silva, J. S., Vicente, J., Ortiz, L., Fernandes, P. M., & Castro-Díez, P. (2020). Assessing the drivers and the recruitment potential of *Eucalyptus globulus* in the Iberian Peninsula. *Forest Ecology and Management*, 466, 118147. <https://doi.org/10.1016/j.foreco.2020.118147>
- Rabasa, S. G., Granda, E., Benavides, R., Kunstler, G., Espelta, J. M., Ogaya, R., ... Valladares, F. (2013). Disparity in elevational shifts of European trees in response to recent climate warming. *Global Change Biology*, 19(8), 2490–2499. <https://doi.org/10.1111/gcb.12220>
- Raz-Yaseef, N., Yakir, D., Schiller, G., & Cohen, S. (2012). Dynamics of evapotranspiration partitioning in a semi-arid forest as affected by temporal rainfall patterns. *Agricultural and Forest Meteorology*, 157, 77–85. <https://doi.org/10.1016/j.agrformet.2012.01.015>
- Rodell, M., Houser, P. R., Jambor, U., Gottschalck, J., Mitchell, K., Meng, C.-J., ... Toll, D. (2004). The global land data assimilation system. *Bulletin of the American Meteorological Society*, 85(3), 381–394. <https://doi.org/10.1175/BAMS-85-3-381>
- Rodríguez-Rodríguez, D., & Martínez-Vega, J. (2018). Protected area effectiveness against land development in Spain. *Journal of Environmental Management*, 215, 345–357. <https://doi.org/10.1016/j.jenvman.2018.03.011>
- Roman, D. T., Novick, K. A., Brzostek, E. R., Dragoni, D., Rahman, F., & Phillips, R. P. (2015). The role of isohydric and anisohydric species in determining ecosystem-scale response to severe drought. *Oecologia*, 179(3), 641–654. <https://doi.org/10.1007/s00442-015-3380-9>
- Ruiz-Benito, P., Lines, E. R., Gómez-Aparicio, L., Zavala, M. A., & Coomes, D. A. (2013). Patterns and drivers of tree mortality in Iberian forests: Climatic effects are modified by competition. *PLoS One*, 8(2). <https://doi.org/10.1371/journal.pone.0056843>
- Ruiz-Labourdette, D., Nogués-Bravo, D., Ollero, H. S., Schmitz, M. F., & Pineda, F. D. (2012). Forest composition in Mediterranean mountains is projected to shift along the entire elevational gradient under climate change. *Journal of Biogeography*, 39(1), 162–176. <https://doi.org/10.1111/j.1365-2699.2011.02592.x>
- Sade, N., Gebremedhin, A., & Moshellon, M. (2012). Risk-taking plants. *Plant Signaling & Behavior*, 7(7), 767–770. <https://doi.org/10.4161/psb.20505>
- Savi, T., Casolo, V., Dal Borgo, A., Rosner, S., Torboli, V., Stenni, B., ... Nardini, A. (2019). Drought-induced dieback of *Pinus nigra*: A tale of hydraulic failure and carbon starvation. *Conservation Physiology*, 7. <https://doi.org/10.1093/conphys/coz012>
- Scarascia-Mugnozza, G., Oswald, H., Piussi, P., & Radoglou, K. (2000). Forests of the Mediterranean region: Gaps in knowledge and research needs. *Forest Ecology and Management*, 132, 97–109.
- Schwalm, C. R., Anderegg, W. R. L., Michalak, A. M., Fisher, J. B., Biondi, F., Koch, G., ... Tian, H. (2017). Global patterns of drought recovery. *Nature*, 548(7666), 202–205. <https://doi.org/10.1038/nature23021>
- Schwartz, N. B., Budsock, A. M., & Uriarte, M. (2019). Fragmentation, forest structure, and topography modulate impacts of drought in a tropical forest landscape. *Ecology*, 100(6), e02677. <https://doi.org/10.1002/ecy.2677>
- Serra-Maluquer, X., Mencuccini, M., & Martínez-Vilalta, J. (2018). Changes in tree resistance, recovery and resilience across three successive extreme droughts in the northeast Iberian Peninsula. *Oecologia*, 187(1), 343–354. <https://doi.org/10.1007/s00442-018-4118-2>
- Sevanto, S., McDowell, N. G., Dickman, L. T., Pangle, R., & Pockman, W. T. (2014). How do trees die? A test of the hydraulic failure and carbon starvation hypotheses. *Plant, Cell & Environment*, 37(1), 153–161. <https://doi.org/10.1111/pce.12141>
- Simonson, W. D., Allen, H. D., & Coomes, D. A. (2012). Use of an airborne lidar system to model plant species composition and diversity of Mediterranean oak forests. *Conservation Biology*, 26(5), 840–850. <https://doi.org/10.1111/j.1523-1739.2012.01869.x>
- Simonson, W., Ruiz-Benito, P., Valladares, F., & Coomes, D. (2016). Modelling above-ground carbon dynamics using multi-temporal airborne lidar: Insights from a Mediterranean woodland. *Biogeosciences*, 13(4), 961–973. <https://doi.org/10.5194/bg-13-961-2016>

- Slette, I. J., Post, A. K., Awad, M., Even, T., Punzalan, A., Williams, S., ... Knapp, A. K. (2019). How ecologists define drought, and why we should do better. *Global Change Biology*, 25(10), 3193–3200. <https://doi.org/10.1111/gcb.14747>
- Slik, J. W. F. (2004). El Niño droughts and their effects on tree species composition and diversity in tropical rain forests. *Oecologia*, 141(1), 114–120. <https://doi.org/10.1007/s00442-004-1635-y>
- Sohn, J. A., Hartig, F., Kohler, M., Huss, J., & Bauhus, J. (2016). Heavy and frequent thinning promotes drought adaptation in *Pinus sylvestris* forests. *Ecological Applications*, 26(7), 2190–2205. <https://doi.org/10.1002/eap.1373>
- Stereńczak, K., Mielcarek, M., Modzelewska, A., Kraszewski, B., Fassnacht, F. E., & Hilszczański, J. (2019). Intra-annual *Ips typographus* outbreak monitoring using a multi-temporal GIS analysis based on hyperspectral and ALS data in the Białowieża Forests. *Forest Ecology and Management*, 442, 105–116. <https://doi.org/10.1016/j.foreco.2019.03.064>
- Tejedor, E., de Luis, M., Cuadrat, J. M., Esper, J., & Saz, M. Á. (2016). Tree-ring-based drought reconstruction in the Iberian Range (east of Spain) since 1694. *International Journal of Biometeorology*, 60(3), 361–372. <https://doi.org/10.1007/s00484-015-1033-7>
- Tucker, C. J., & Sellers, P. J. (1986). Satellite remote sensing of primary production. *International Journal of Remote Sensing*, 7(11), 1395–1416. <https://doi.org/10.1080/01431168608948944>
- Turco, M., Herrera, S., Tourigny, E., Chuvieco, E., & Provenzale, A. (2019). A comparison of remotely-sensed and inventory datasets for burned area in Mediterranean Europe. *International Journal of Applied Earth Observation and Geoinformation*, 82, 101887. <https://doi.org/10.1016/j.jag.2019.05.020>
- Turner, D. P., Cohen, W. B., Kennedy, R. E., Fassnacht, K. S., & Briggs, J. M. (1999). Relationships between leaf area index and landsat TM spectral vegetation indices across three temperate zone sites. *Remote Sensing of Environment*, 70(1), 52–68. [https://doi.org/10.1016/S0034-4257\(99\)00057-7](https://doi.org/10.1016/S0034-4257(99)00057-7)
- UNEP/MAP. (2016). *Mediterranean strategy for sustainable development 2016–2025*. Valbonne, France: Plan Bleu, Regional Activity Centre. [https://wedocs.unep.org/bitstream/handle/20.500.11822/7700/-Mediterranean\\_strategy\\_for\\_sustainable\\_development\\_2016-2025\\_investing\\_in\\_environmental\\_sustainability\\_to\\_achieve\\_social\\_and\\_economic\\_development-20.pdf?sequence=3](https://wedocs.unep.org/bitstream/handle/20.500.11822/7700/-Mediterranean_strategy_for_sustainable_development_2016-2025_investing_in_environmental_sustainability_to_achieve_social_and_economic_development-20.pdf?sequence=3)
- Valladares, F., Matesanz, S., Guilhaumon, F., Araújo, M. B., Balaguer, L., Benito-Garzon, M., ... Zavala, M. A. (2014). The effects of phenotypic plasticity and local adaptation on forecasts of species range shifts under climate change. *Ecology Letters*, 17(11), 1351–1364. <https://doi.org/10.1111/ele.12348>
- Vayreda, J., Gracia, M., Martinez-Vilalta, J., & Retana, J. (2013). Patterns and drivers of regeneration of tree species in forests of peninsular Spain. *Journal of Biogeography*, 40(7), 1252–1265. <https://doi.org/10.1111/jbi.12105>
- Verbesselt, J., Hyndman, R., Newnham, G., & Culvenor, D. (2010). Detecting trend and seasonal changes in satellite image time series. *Remote Sensing of Environment*, 114, 106–115. <https://doi.org/10.1016/j.rse.2009.08.014>
- Verbesselt, J., Robinson, A., Stone, C., & Culvenor, D. (2009). Forecasting tree mortality using change metrics derived from MODIS satellite data. *Forest Ecology and Management*, 258(7), 1166–1173. <https://doi.org/10.1016/J.FORECO.2009.06.011>
- Vicente-Serrano, S. M., Azorin-Molina, C., Sanchez-Lorenzo, A., Morán-Tejeda, E., Lorenzo-Lacruz, J., Revuelto, J., ... Espejo, F. (2014). Temporal evolution of surface humidity in Spain: Recent trends and possible physical mechanisms. *Climate Dynamics*, 42, 2655–2674. <https://doi.org/10.1007/s00382-013-1885-7>
- Vicente-Serrano, S. M., Beguería, S., & López-Moreno, J. I. (2010). A multiscalar drought index sensitive to global warming: The standardized precipitation evapotranspiration index. *Journal of Climate*, 23(7), 1696–1718. <https://doi.org/10.1175/2009JCLI2909.1>
- Vicente-Serrano, S. M., Gouveia, C., Camarero, J. J., Beguería, S., Trigo, R., Lopez-Moreno, J. I., ... Sanchez-Lorenzo, A. (2013). Response of vegetation to drought time-scales across global land biomes. *Proceedings of the National Academy of Sciences of the United States of America*, 110(1), 52–57. <https://doi.org/10.1073/PNAS.1207068110>
- Vicente-Serrano, S. M., Lopez-Moreno, J.-I., Beguería, S., Lorenzo-Lacruz, J., Sanchez-Lorenzo, A., García-Ruiz, J. M., ... Espejo, F. (2014). Evidence of increasing drought severity caused by temperature rise in southern Europe. *Environmental Research Letters*, 9(4), 044001. <https://doi.org/10.1088/1748-9326/9/4/044001>
- Vicente-Serrano, S. M., Tomas-Burguera, M., Beguería, S., Reig, F., Latorre, B., Peña-Gallardo, M., ... González-Hidalgo, J. C. (2017). A high resolution dataset of drought indices for Spain. *Data*, 2(3), 22. <https://doi.org/10.3390/data2030022>
- Villaescusa, R., & Díaz, R. (1998). *Segundo Inventario Forestal Nacional (1986–1996)*. Madrid, Spain: Ministerio de Medio Ambiente.
- Villanueva, J. A. (2004). *Tercer Inventario Forestal Nacional (1997–2007)*. Madrid, Spain: Ministerio de Medio Ambiente.
- Yin, J., & Bauerle, T. L. (2017). A global analysis of plant recovery performance from water stress. *Oikos*, 126(10), 1377–1388. <https://doi.org/10.1111/oik.04534>
- Zhang, X., Friedl, M. A., Schaaf, C. B., Strahler, A. H., Hodges, J. C. F., Gao, F., ... Huete, A. (2003). Monitoring vegetation phenology using MODIS. *Remote Sensing of Environment*, 84(3), 471–475. [https://doi.org/10.1016/S0034-4257\(02\)00135-9](https://doi.org/10.1016/S0034-4257(02)00135-9)
- Zhu, Z., Piao, S., Myneni, R. B., Huang, M., Zeng, Z., Canadell, J. G., ... Zeng, N. (2016). Greening of the Earth and its drivers. *Nature Climate Change*, 6(8), 791–795. <https://doi.org/10.1038/NCLIMATE3004>

## SUPPORTING INFORMATION

Additional supporting information may be found online in the Supporting Information section.

**How to cite this article:** Khoury S, Coomes DA. Resilience of Spanish forests to recent droughts and climate change. *Glob Change Biol*. 2020;26:7079–7098. <https://doi.org/10.1111/gcb.15268>